

# Screening 0D materials for 2D nanoelectronics applications

Mohammad Bagheri Hannu-Pekka Komsa\*

M. Bagheri, Prof. H.-P. Komsa

Microelectronics Research Unit, University of Oulu, P.O. Box 8000, 90014 Oulu, Finland

Email Address: hannu-pekka.komsa@oulu.fi

Keywords: *0D materials, database screening, density-functional theory, nanoelectronics*

As nanoelectronic devices based on two-dimensional (2D) materials are moving towards maturity, optimization of the properties of the active 2D material must be accompanied by equal attention to optimizing the properties of and the interfaces to the other materials around it, such as electrodes, gate dielectrics, and the substrate. While these are usually either 2D or 3D materials, recently K. Liu *et al.* [Nat. Electron. 4, 906 (2021)] reported on the use of zero-dimensional (0D) material, consisting of vdW-bonded  $\text{Sb}_2\text{O}_3$  clusters, as a highly promising insulating substrate and gate dielectric. Here, we report on computational screening study to find promising 0D materials for use in nanoelectronics applications, in conjunction with 2D materials in particular. By combining a database and literature searches, we found 16 materials belonging to 6 structural prototypes with high melting points and high band gaps, and a range of static dielectric constants. We carried out additional first-principles calculations to evaluate selected technologically relevant material properties, and confirmed that all these materials are van der Waals-bonded, thus allowing for facile separation of 0D clusters from the 3D host and also weakly perturbing the electronic properties of the 2D material after deposition.

## 1 Introduction

Two-dimensional (2D) materials are widely investigated for use in nanoelectronics devices, especially as an ultrathin channel in next-generation field-effect transistors and novel logic architectures [1, 2, 3], memory cells [4, 5], memristors [6, 7], rectenna [8], and others [9]. In all of these applications, one needs to optimize not only the properties of the “active” 2D material, but also all the other materials around it, such as the dielectrics, electrodes, and substrate, and the material interfaces between them. In a wide majority of cases, either other 2D materials or common 3D materials are used for these purposes. Recently, formation of 2D molecular crystal was demonstrated from  $\text{Sb}_2\text{O}_3$  0D material, i.e., a material consisting of weakly bound small molecular units with no dangling bonds [10]. Using these as a substrate or gate dielectric in 2D material field-effect transistors resulted in high mobility, small hysteresis, low density of trap states, and high subthreshold slope [11]. The authors called for theoretical studies to find more suitable 0D material candidates [11, 12].

While 2D and 1D materials have been searched in many previous publications by screening experimental and/or computational material databases [13, 14, 15, 16], to the best of our knowledge, not 0D materials. While 0D materials are easily identified using the same dimensionality identification methods, many of the found materials are crystalline phases of substances that are gaseous or liquid even in atmospheric conditions, and thus not useable in the above-mentioned applications. Finding the materials that are crystalline at technologically relevant temperatures requires estimating the melting points, which is computationally highly demanding.

In this Letter, we take first steps in identifying a set of promising 0D materials for use in electronics applications, as a substrate or as a gate dielectric. We achieve this by combining screening of the Materials Project database and supplementing it by manual pruning of the list, most importantly by extracting experimental melting points from the literature. We identified 16 materials belonging to 6 structural prototypes with high melting points and high band gaps, and both high and low dielectric constants. We performed van der Waals density-functional theory calculations to evaluate selected material properties and also studied their interaction with the prototypical 2D material  $\text{MoS}_2$ .

## 2 Results

### 2.1 Database screening

We start by performing a database search to Materials Project (MP) [17], as illustrated in Fig. 1(a), with the following search criteria

Cr1 The structure is classified to have 0D dimensionality.

Cr2 The structure consist of only one type of 0D cluster and the size of the cluster is larger than 3 atoms.

Cr3 Energy above convex hull  $E_{\text{hull}}$  is less than 0.1 eV/atom.

Cr4 The MP entry contains calculated dielectric constant.

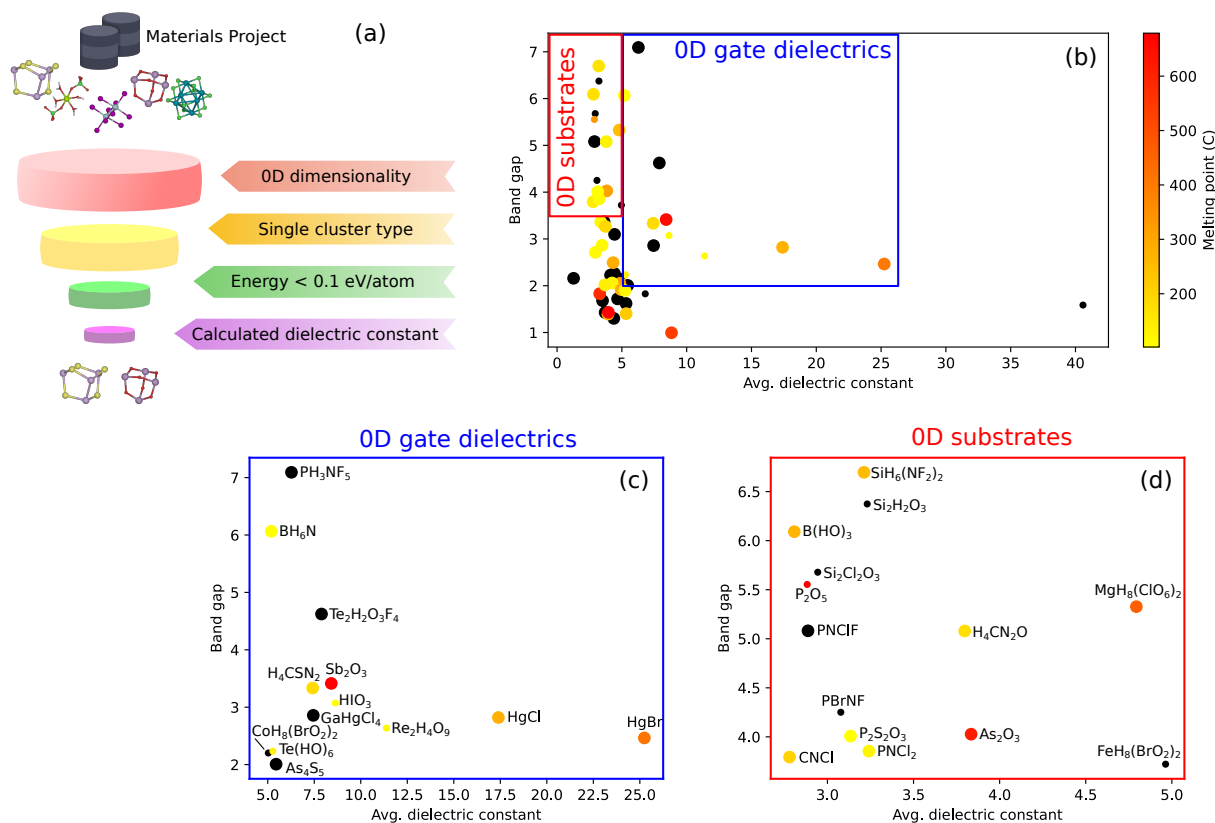


Figure 1: (a) Schematic representation of the materials database screening procedure. (b-d) Band gap vs. average static dielectric constant from (b) all 56 materials with melting point above 100 °C, (c) materials with band gap larger than 2 and dielectric constant larger than 5, and (d) materials with band gap larger than 3.5 and dielectric constant less than 5. Marker color indicates the melting point (see colorbar, or black if not known). Large/small marker size indicate that the material is stable/unstable, defined as the energy above convex hull being less/more than 10 meV/atom.

Several approaches have been proposed for the classification of structure dimensionality [18, 14, 19]. We are using the algorithm proposed by Larsen *et al.* [19], which also gives a useful measure of the degree of “0D-ness”. Upon applying Cr1, out of 126335 materials in MP (accessed on 25th Jan 2022), 8335 were identified as 0D materials.

Criterion Cr2 is chosen for simplicity and since deposition of materials consisting of many different clusters can be difficult to control, especially since the deposition is ideally carried out at a relatively low temperature. The clusters are compared only by the formula (number and types of atoms in the cluster), not their atomic structures. Application of this criterion (on top of Cr1) yields 2395 materials. In addition, we have required that the number of atoms in the cluster is larger than 3. Clusters with one atom can be trivially ignored (mostly noble gases), and most systems with 2- or 3-atom clusters correspond to solid phases of, e.g., hydrogen halides (HF, HCl, etc.) or simple molecules such as N<sub>2</sub>, H<sub>2</sub>O, and CO<sub>2</sub>. It is unlikely that very promising new 0D materials can be found among these. Finally, we have required that the “0D-ness” dimensionality score used in the classification scheme is higher than 0.8 [19]. The threshold was found by manually inspecting the structures with lowest score and comparing the dimensionality to that reported in MP. The materials with low dimensionality score are borderline between different dimensionalities and usually indicates that the bonding between the (nearly) 0D clusters is stronger than in purely vdW-bonded systems. Application of these criteria yields 1965 materials.

Applying the energy criterion Cr3, reduces the number of material candidates by about a factor of two to 942.

Finally, in the last step of our database screening, criterion Cr4 yields a marked reduction in the number of entries, down to 162. These materials are listed in Table S1. Omitting such a large number of entries (780) may appear unwarranted, but we will revisit this group of materials later in this paper.

In the next stage, we manually pruned the list. First, if several phases of same material are found, we retain only the lowest energy phase, down to 138 materials. Inspection of the list also indicates that many of these materials are liquid or gaseous under atmospheric conditions (e.g., methane, ammonia, and various acids). In order to find materials with stable crystalline structure at moderate processing temperatures, we collected experimentally measured melting points for all materials where we could find one (also listed in Table S1). After removing the materials that are known to be liquid or gas under typical operating temperatures (melting point below 100 °C), we are left with 56 entries.

The band gaps with respect to rotationally averaged static dielectric constants, or “polycrystalline dielectric constant”,  $\epsilon_{\text{poly}}^0$  for these 56 materials are plotted in Fig. 1(b). In electronics applications with relatively slowly varying fields, the static dielectric constants are more relevant than the high-frequency one  $\epsilon_{\infty}$ . In fact, the ionic contribution to the dielectric constant is critical for achieving large screening, as evidenced from the plot of the band gap vs.  $\epsilon_{\infty}$  shown in Figure S1.

In order to find materials suitable for use as gate dielectrics, we extract materials with band gap larger than 2 eV and  $\epsilon_{\text{poly}}^0$  larger than 5. The relatively low band-gap threshold was chosen since DFT with semilocal functionals underestimates gaps, sometimes significantly so, by upto a factor of two. In this group, shown in Fig. 1(b), there are only 13 materials, which we analyze in detail. The atomic structures of the corresponding 0D clusters are shown in Fig. S2 (and in Fig. 2 for the promising candidates).

The only material with very high melting point (mp.) is  $\text{Sb}_2\text{O}_3$  (656 °C), that was already previously identified [10, 11]. The atomic structure consists of  $\text{Sb}_4\text{O}_6$  cages, similar to  $\text{C}_{10}\text{H}_{16}$  carbon cages, called adamantane, but without terminating H. There are few materials with higher dielectric constant, such as  $\text{HgBr}$ ,  $\text{HgCl}$ , and  $\text{Re}_2\text{H}_4\text{O}_9$ , but those have also lower band gap and lower melting point. Moreover, although  $\text{HgBr}$  and  $\text{HgCl}$  have fairly high mp., they are unfortunately highly toxic.  $\text{Re}_2\text{H}_4\text{O}_9$  structure is similar to, but not exactly the same as, that of perrhenic acid. It is a metal oxide coordinated with water with mp. of 115 °C, which is likely too low.

Among others (from high to low band gap),  $\text{PH}_3\text{NF}_5$  is a Lewis acid-base adduct, with fairly little experimental data. It has been synthesized, but expected to have low melting point [20].  $\text{BH}_6\text{N}$  has a low mp. of 104 °C. No mp. was found for  $\text{Te}_2\text{H}_2\text{O}_3\text{F}_4$ , but stable at room temperature and computationally stable.  $\text{H}_4\text{CSN}_2$ , thiourea, has mp. of 182 °C, making it possibly interesting.  $\text{HIO}_3$ , iodic acid, has band gap and dielectric constant close to  $\text{Sb}_2\text{O}_3$ , but the mp. of 110 °C is again low.  $\text{GaHgCl}_4$  has been synthesized and is computationally stable. No mp. was found and it is sensitive to humidity [21].  $\text{CoH}_8(\text{BrO}_2)_2$  (or  $\text{CoBr}_2(\text{H}_2\text{O})_4$ ) consist of hydrated  $\text{CoBr}_2$  molecules. The degree of hydration is sensitive to temperature between 0-100 °C[22], which may prove problematic in applications. We could not find mp., but high  $E_{\text{hull}}$  of 0.053 eV/atom suggests poor stability.  $\text{Te}(\text{HO})_6$ , telluric acid, has mp. of 136 °C, which is likely too low. Finally,  $\text{As}_4\text{S}_5$  is a rare mineral called uzonite [23]. It is related to another mineral  $\text{As}_4\text{S}_4$ , realgar, also with fairly similar cage-like structure, and mp. 320 of °C. Thus, although the band gap and dielectric constant are fairly low, the cage-like structure and stability of arsenic sulfides makes them promising.

Eventually, the number of viable candidates found by this screening is small. In addition to  $\text{Sb}_2\text{O}_3$ , there are only  $\text{As}_4\text{S}_5$  (and maybe very similar  $\text{As}_4\text{S}_4$ ) (uzonite/realgar). The commonness of thiourea could make it interesting in some cases.

For use as a substrate, the band gap is often more important than the dielectric constant. Low dielectric constant materials (low- $\kappa$  dielectrics) are also used in separating the interconnects in circuits, to reduce crosstalk and parasitic capacitance. Moreover, in optoelectronic applications low dielectric constant might be desired in order to minimize screening by the substrate and to avoid subsequent renormalization of fundamental band gap and/or reduction in exciton binding energy [24, 25, 26, 27]. We next focus on the large band gap ( $> 3.5$  eV) but small dielectric constant materials  $\epsilon_{\text{poly}}^0 < 5$ , which yields 14 materi-

als shown in Figure 1(d) and the structures in Fig. S3. Two interesting candidates can be immediately pinpointed:  $\text{As}_2\text{O}_3$  and  $\text{P}_2\text{O}_5$ .  $\text{As}_2\text{O}_3$  has the same structure as  $\text{Sb}_2\text{O}_3$ , i.e., belonging to adamantanes. It has mp. of 312 °C and is also found as a mineral arsenolite (and in small quantities in arsenic sulfide minerals uzonite and realgar mentioned above).  $\text{P}_2\text{O}_5$  is also reminiscent of adamantanes but with additional terminating oxo groups. It has mp. 340 °C, and while this polymorph consisting of  $\text{P}_4\text{O}_{10}$  molecules is in principle metastable, it is nevertheless commonly encountered. We note that  $\text{P}_2\text{S}_2\text{O}_3$  consists of  $\text{P}_4\text{O}_6\text{S}_4$  clusters similar to  $\text{P}_2\text{O}_5$  but the tip O replaced by S. However, it has much lower mp. of 102 °C.

Highest band gaps are found from silicon clusters.  $\text{SiH}_6(\text{NF}_2)_2$  is an adduct of  $\text{SiF}_4$  and  $2\text{NH}_3$  and computationally stable, although mp. of only 166 °C.  $\text{Si}_2\text{H}_2\text{O}_3$  and  $\text{Si}_2\text{Cl}_2\text{O}_3$  cluster both have pyramidal structure consisting of four formula units, similar to  $\text{P}_4\text{O}_{10}$ . We did not find mp., but  $E_{\text{hull}} = 0.023$  and  $E_{\text{hull}} = 0.026$  eV/atom, respectively, suggests fairly poor stability. Highest dielectric constants are found from metal halogen compounds.  $\text{FeH}_8(\text{BrO}_2)_2$  has a structure similar to  $\text{CoH}_8(\text{BrO}_2)_2$  [28], and is similarly sensitive to humidity and exhibits fairly poor stability with  $E_{\text{hull}} = 0.026$  meV/atom.  $\text{MgH}_8(\text{ClO}_6)_2$  (or  $\text{Mg}(\text{ClO}_4)_2(\text{H}_2\text{O})_4$ ) is a hydrated version of magnesium perchlorate, which is a strong drying agent, which may again prove problematic. On the other hand, it has fairly high mp. of 251 °C and computationally stable.

Otherwise,  $\text{B}(\text{HO})_3$ , boric acid, has mp. 171 °C, and is also found in mineral sassolite, but dissolves in water.  $\text{H}_4\text{CN}_2\text{O}$ , urea, has mp. of only 133 °C and thiourea has overall better properties.  $\text{PNCl}_2$  is phosphazene with 6-membered ring with alternating P and N, but mp. of 112 °C is too low.  $\text{PNCIF}$  and  $\text{PBrNF}$  are similar and, though they are stable at RT, the mp. is likely low as in other phosphorus halides [29].  $\text{CNCl}$ , cyanuric chloride, consists of 6-membered ring with alternating C and N, and has mp. of 144 °C. Thus, from this set, we found only two clearly promising materials to be used as a substrate:  $\text{As}_2\text{O}_3$ ,  $\text{P}_2\text{O}_5$ . Possibly interesting candidates are magnesium perchlorate and boric acid.

Finally, it is worth highlighting few specific data points in Fig. 1(b). The material with dielectric constant over 40 is  $\text{H}_2\text{Pt}(\text{OH})_6$ , platinic acid. In crystalline form, it is experimentally stable to about 150 °C, after which it starts to form  $\text{PtO}_2$  [30]. The calculated  $E_{\text{hull}} = 0.069$  eV/atom also suggests poor stability. There are also three high melting point materials, shown by red markers, in Fig. 1(b):  $\text{PtCl}_2$ ,  $\text{PdCl}_2$ , and  $\text{NbI}_5$ . The Pt and Pd chlorides in  $\beta$ -phase consist of octahedral cage structure with six formula units (hexamer).  $\text{PtCl}_2$  and  $\text{PdCl}_2$  are reported to have high mp. of 581 and 679 °C, respectively, but those values correspond to the polymeric  $\alpha$ -phase. There is a phase transition from  $\beta$ - to  $\alpha$ -phase at around 500 °C [31], which is still high. The calculated band gaps are less than 2 eV and dielectric constant 3–4.  $\text{NbI}_5$  is a molecular dimer with mp. 543 °C, gap 1.0 eV, and  $\epsilon_{\text{poly}}^0 = 8.8$ .

From this database search, we have ended up with 8 materials in 6 cluster prototypes that showed high melting points and reasonably high band gap and dielectric constant: adamantane ( $\text{Sb}_4\text{O}_6$ ,  $\text{As}_4\text{O}_6$ ), uzonite ( $\text{As}_4\text{S}_5$ ), realgar ( $\text{As}_4\text{S}_4$ ) terminated adamantane (denoted T-adamantane,  $\text{P}_4\text{O}_{10}$ ), metal halide hexamer (MH-hexamer,  $\text{Pt}_6\text{Cl}_{12}$ ,  $\text{Pd}_6\text{Cl}_{12}$ ), and metal halide dimer (MH-dimer,  $\text{Nb}_2\text{I}_{10}$ ). The prototype cluster structures are visualized in Fig. 2.

We now revisit the materials for which calculated dielectric constant was not available in MP. We represented all cluster structures as connected graphs and then searched for graphs that are isomorphic to the prototype systems among those where dielectric constant was not available. We stress, that this approach only considers the connectivity/bonding network between atoms, but ignores the atom types and thus, for example,  $\text{P}_4\text{O}_{10}$  and  $\text{P}_4\text{S}_4\text{O}_6$  are isomorphic despite having only a fraction of the oxygens replaced by sulfur. This search yielded in total 27 structures, 3 adamantanes, 1 uzonite-like, 2 realgar-like, 3 T-adamantanes, 0 MH-hexamer, 18 MH-dimer. These are listed in Table S2. We again pruned the list by removing low mp. and metastable systems, and those with zero or vanishingly small band gap. It is worth noting that four of the metal halide dimers with zero band gap also exhibited nonzero magnetic moment. We are left with 12 additional materials: uzonite-like  $\text{As}_4\text{Se}_4$  with mp. of 265 °C; T-adamantane  $\text{P}_4\text{S}_{10}$ ,  $\text{Ge}_4\text{S}_6\text{Br}_4$ ,  $\text{Ge}_4\text{S}_6\text{I}_4$  all have mp close to 300 °C; MH-dimers  $\text{Nb}_2\text{Br}_{10}$  and  $\text{Ta}_2\text{Br}_{10}$  have mp. 250–300 °C,  $\text{Nb}_2\text{Cl}_{10}$  has mp. close to 200 °C, and  $\text{Ta}_2\text{I}_{10}$  has mp. of 382 °C.

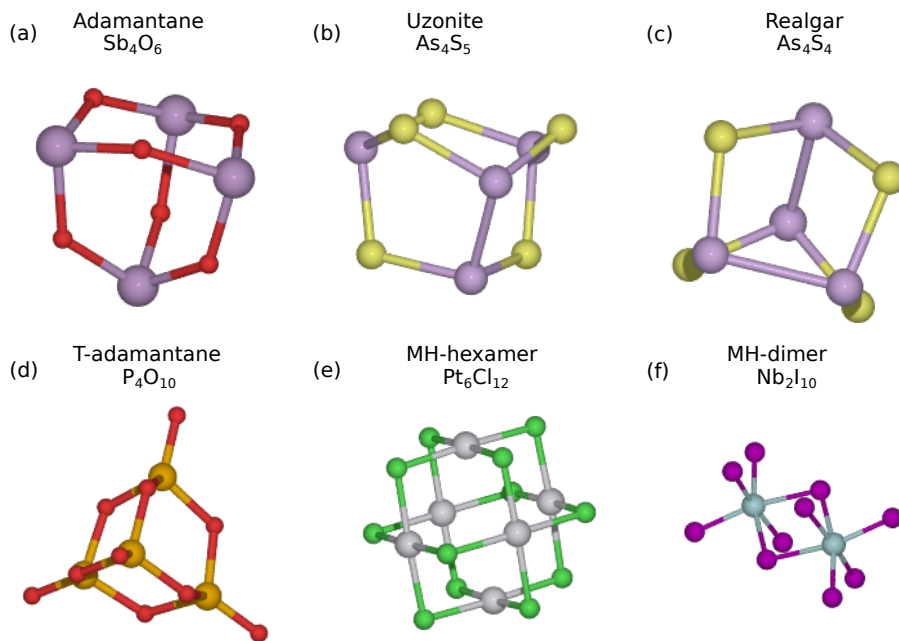


Figure 2: Atomic structures of the cluster prototypes.

## 2.2 Cluster properties

From the screening study presented thus far, we are left with 16 materials in the 6 prototypes. Since Materials Project data is calculated using PBE functional that poorly describes van der Waals interactions, we recalculated these systems, both crystalline and isolated clusters, using vdW-DF functional. Selected properties are collected in Table 1, such as binding energies, band gaps and dielectric constants, and additional properties are listed in Table S3. The experimental melting point is also included for convenience in Table 1.

The binding energies per cluster are usually few eVs, which may appear quite large, but the sizes of these clusters and the areas between them are also significant. We estimate binding energy per area by mapping the volume per molecule in a crystal to a sphere and taking its area. These values fall within 6–40 meV/Å, which is comparable to the 2D material binding energies, where majority of compounds fall within 13–21 meV/Å [32, 33]. Thus, it appears safe to label these systems as vdW-bonded 0D materials. In Table 1, we also listed the gaps calculated using vdW-DF for crystals and for isolated clusters. Comparing to the MP gaps listed in Tables S1 and S2, shows that, as van der Waals interaction pulls the clusters closer together, the band gap decreases: 0.4–0.5 eV decrement is seen for many materials, except for  $\text{As}_2\text{O}_3$  and  $\text{P}_2\text{O}_5$  which remain largely unaffected. The lowering of the band gap is in turn reflected in slight increase of the dielectric constants, see also the plot of band gap vs. dielectric constant shown in Fig. 3(a). Conversely, the HOMO-LUMO gaps of the isolated clusters are higher than the crystal gaps by about 0.5–1 eV.

For nanoelectronics applications, it is important to know the alignment of the valence band maxima and conduction band minima of the 0D materials with respect to the band extrema of the 2D materials. Here, we evaluated this from the HOMO and LUMO levels of isolated clusters and the results are shown in Fig. 3(b). Adamantanes, uzonite, realgars, and some of T-adamantanes have all suitable band edge positions compared to common 2D materials. Metal halide hexamer and dimer band edges are deep and as a result the LUMO level of 0D cluster are below the conduction band minima of most 2D materials. 0D materials have several natural cleaving planes, that lead to 2D layers of clusters with different orientations and different lattices, depending on the symmetry of the clusters and of the 3D lattice. It is not *a priori* clear what will be the preferred orientation and ordering of the clusters when sputtered on top of a particular 2D material and how to control the growth mode [12]. Investigating this by first-principles calculations is highly demanding.

Table 1: Selected properties of promising 0D materials calculated using vdW-DF functional: cluster formula, binding energy per area (meV/Å), band gap from crystal (eV), HOMO-LUMO gap from cluster (eV), and static and high-frequency dielectric constants. The experimental melting points (mp., in °C) are also included for convenience.

formula	binding energy	mp.	Crystal gap	Cluster gap	$\epsilon_{\text{poly}}^{\infty}$	$\epsilon_{\text{poly}}^0$
Sb <sub>4</sub> O <sub>6</sub>	-30.37	656.0	2.92	4.09	3.95	10.92
As <sub>4</sub> S <sub>5</sub>	-18.66		1.42	2.64	6.31	8.10
As <sub>4</sub> S <sub>4</sub>	-17.29	320.0	1.38	2.80	6.80	7.91
As <sub>4</sub> O <sub>6</sub>	-18.30	312.2	4.04	4.49	2.59	4.92
P <sub>4</sub> O <sub>10</sub>	-13.40	340.0	5.47	6.01	1.37	2.41
Pt <sub>6</sub> Cl <sub>12</sub>	-6.15	581.0	1.48	2.01	3.99	4.19
Pd <sub>6</sub> Cl <sub>12</sub>	-6.50	679.0	1.09	1.64	6.25	6.80
Nb <sub>2</sub> I <sub>10</sub>	-8.04	543.0	0.61	1.08	9.98	15.01
As <sub>4</sub> Se <sub>4</sub>	-39.87	265.0	0.85	2.17	10.69	12.61
P <sub>4</sub> S <sub>10</sub>	-12.33	288.0	2.17	2.97	3.98	4.60
Ge <sub>4</sub> S <sub>6</sub> Br <sub>4</sub>	-11.46	305.0	2.14	2.79	3.40	4.22
Ge <sub>4</sub> S <sub>6</sub> I <sub>4</sub>	-11.02	310.0	2.06	2.59	3.85	4.75
Nb <sub>2</sub> Br <sub>10</sub>	-26.47	254.0	1.37	1.70	4.72	7.13
Ta <sub>2</sub> Br <sub>10</sub>	-18.94	265.0	1.86	2.19	3.85	5.79
Nb <sub>2</sub> Cl <sub>10</sub>	-17.27	204.7	2.07	2.33	3.12	4.99
Ta <sub>2</sub> I <sub>10</sub>	-30.31	382.0	0.94	1.41	7.25	10.54

To shed light on the interaction of the clusters with 2D materials, we first studied the interaction of isolated 0D clusters placed on a monolayer MoS<sub>2</sub>. The density of states for all 16 cases are collected in Fig. S4 and shows that the MoS<sub>2</sub> states are largely unaffected by the 0D cluster, evidencing that the interaction is weak. Moreover, in Fig. S4 we also indicate the binding energies. For the interaction area we have again transformed the volume per cluster to a sphere (as mentioned above) and taken its great circle. The values fall within 10–20 meV/Å, again similar to those reported above and as reported for many 2D materials, providing evidence to the vdW-type binding with the 2D material.

Next, as an example, we constructed one heterostructure with the surface of WSe<sub>2</sub> fully covered by As<sub>2</sub>O<sub>3</sub>. Due to the similarity of As<sub>2</sub>O<sub>3</sub> and Sb<sub>2</sub>O<sub>3</sub>, the structure of 0D clusters on the surface is also likely similar, and thus we can adopt for As<sub>2</sub>O<sub>3</sub> the experimentally determined structure of Sb<sub>2</sub>O<sub>3</sub>. For the 2D material we chose WSe<sub>2</sub> due to suitable lattice constant, which allowed us to construct heterostructure model with minimal strain. As<sub>2</sub>O<sub>3</sub> has higher band gap than Sb<sub>2</sub>O<sub>3</sub> but smaller dielectric constant and thus useful as a low- $\kappa$  dielectric or, e.g., as a substrate for studying single-photon emitters in WSe<sub>2</sub> [34, 35] without interference from the substrate defects. The optimized atomic structure is shown in Fig. 3(c). The atomic structures of both the WSe<sub>2</sub> and As<sub>2</sub>O<sub>3</sub> layers are very weakly perturbed by the neighboring layer, indicating again van der Waals type interaction. Similarity of the effective band structure of the heterostructure and the band structure of pristine WSe<sub>2</sub> in Fig. 3(d) demonstrates that the band structures of As<sub>2</sub>O<sub>3</sub> and WSe<sub>2</sub> are effectively uncoupled. The As<sub>2</sub>O<sub>3</sub> bands with very small dispersion are seen at about 2 eV below valence band maximum and about 1 eV above conduction band minimum of WSe<sub>2</sub>. Thus, charge transfer to/from the As<sub>2</sub>O<sub>3</sub> should not occur and we expect the electronic and optical properties of WSe<sub>2</sub> layers to remain largely intact.

### 3 Conclusion

In conclusion, we have extracted a list of promising 0D materials to be used with 2D materials in nano-electronics applications, exhibiting fairly high band gaps, dielectric constants, and melting points. This was achieved by screening Materials Project database, combining it with experimental melting points, and using graph-theoretical methods to find other similar structures. We used first-principles calculations to predict additional material properties and studied the interaction of the 0D clusters with a prototypical 2D materials MoS<sub>2</sub>. All these materials were confirmed to have binding energies typical for vdW-bonded systems and to weakly perturb the electronic structure of the 2D material.

Owing to the vdW gaps between clusters, their conductivity is expected to be low and thus they should

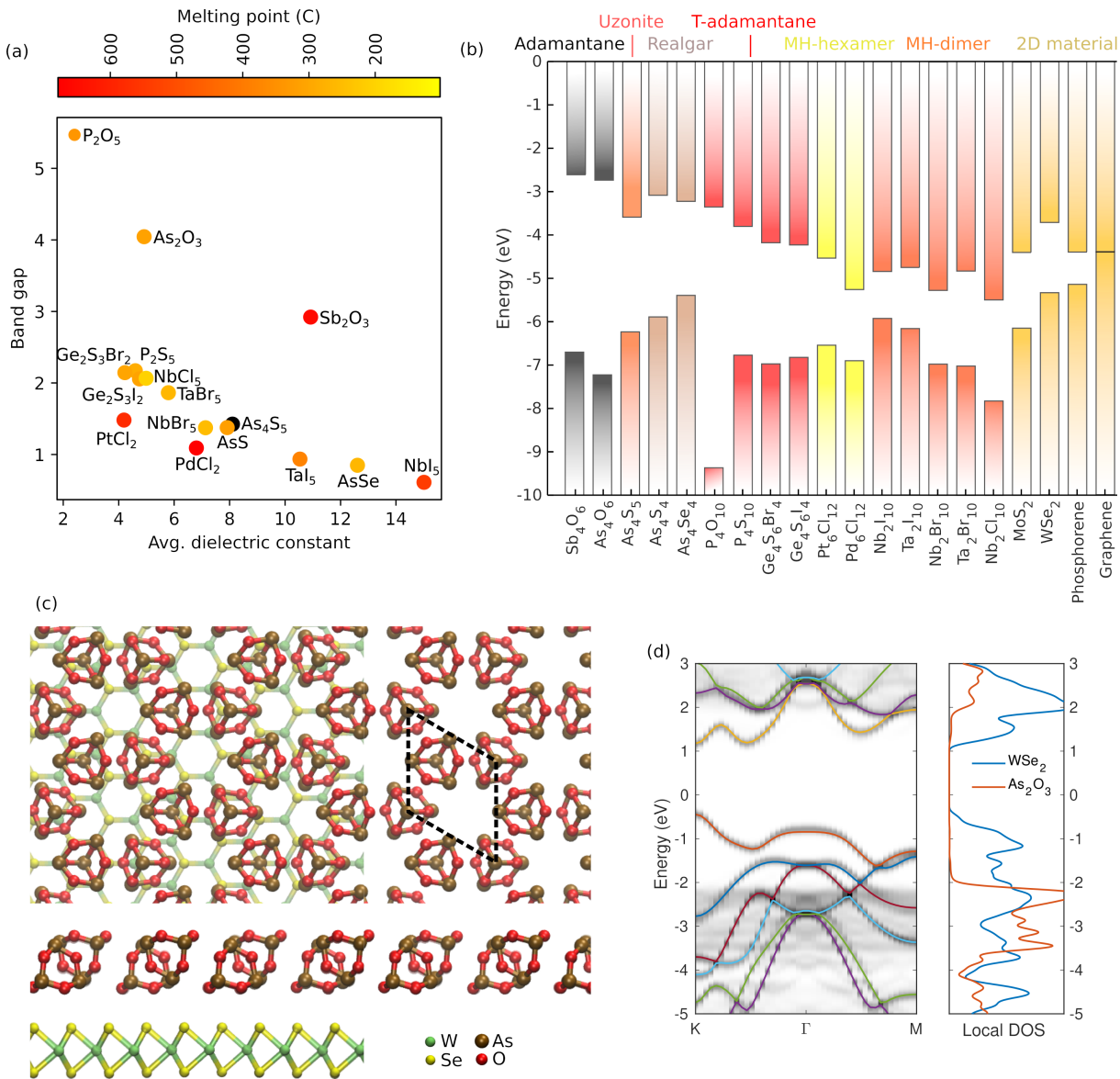


Figure 3: Properties from vdW-DF calculations. (a) Band gap vs. static dielectric constant. Marker color indicates the melting point or black if unknown. (b) HOMO and LUMO levels of 0D clusters aligned via vacuum level. The materials are grouped and colored according to the cluster prototype. (c) Top and side views of atomic structure of  $As_2O_3$  on  $WSe_2$ . Dashed rhombus denotes the  $As_2O_3$  surface unit cell. (d) Effective band structure of the heterostructure model (underlying gray features) compared to the band structure of pristine  $WSe_2$  (overlaid lines). The local DOS of  $As_2O_3$  and  $WSe_2$  layers are also shown.

be fairly good insulators even though their band gaps in the crystalline form are not very high. Consequently, “metallic” 0D materials do not appear particularly promising as electrode materials. In addition to their use as a gate dielectric or substrate, these 0D materials could be used as spacer layers in 2D material superlattices [36]. Intercalation between 2D layers can also stabilize crystalline order for clusters that have too low melting point in 3D lattice. For instance, superlattices of 2D materials and CTAB (and other related) molecules was demonstrated in [37]. Also,  $AlCl_3$  and  $CuCl_2$  clusters and various dimerized and trimerized forms of them have successfully been intercalated between graphene sheets [38]. Although materials consisting of more than one type of clusters were ignored in this Letter for reasons of simplicity, a vast variety of such 0D molecular compounds could exist. As an example, 2D crystal made of  $SbI_3$  and  $S_8$  molecular units was reported in Ref. [39].

We hope that the our study motivates further experimental and computational work on these materials. Based on the cluster prototypes identified here, other 0D materials could be identified or purposefully

designed, either by substitution or by addition of functional groups. These can extend the range of properties or provide even new functionalities, such as charge doping or magnetism.

## 4 Methods

The material information were extracted from Materials Project we used the REST API [40]. The structures were then fed into the dimensionality analysis tools as implemented in ASE [41]. The graph-theoretical part was done using NetWorkX package [42].

All density-functional theory calculations were carried out using VASP software [43, 44], together with projector augmented plane wave method. We adopted Hamada's rev-VDW-DF2 functional [45, 46, 47, 48], which was found to yield good structural properties and interlayer binding energies for 2D materials [33]. Most other input parameters were taken from the Materials Project [17, 40], such as the k-point meshes and the plane wave cutoff of 520 eV. Isolated molecules on MoS<sub>2</sub> were modeled using 4×4 supercell of MoS<sub>2</sub> and a 3×3 k-point mesh. For the heterostructure of As<sub>2</sub>O<sub>3</sub> and WSe<sub>2</sub>, we take the [111] plane of As<sub>2</sub>O<sub>3</sub>. This has lattice constant of 7.715 Å, in which case a 3×3 supercell (23.144 Å) matches closely with a 7×7 supercell of WSe<sub>2</sub> ( $7 \cdot 3.297 = 23.079$  Å). In the heterostructure model, we keep the lattice constant of WSe<sub>2</sub> fixed and compressively strain As<sub>2</sub>O<sub>3</sub> layer by 0.28%. We used 2×2 k-point mesh during relaxation and 4×4 k-point mesh in calculating density of states. Effective band structure was calculated using BandUP code [49].

### Supporting Information

Supporting Information is available from the Wiley Online Library or from the author.

### Acknowledgements

We thank CSC-IT Center for Science Ltd. for generous grants of computer time.

### Conflict of Interest

The authors declare no conflict of interest.

## References

- [1] B. Radisavljevic, A. Radenovic, J. Brivio, V. Giacometti, A. Kis, *Nature Nanotechnology* **2011**, *6*, 3 147.
- [2] C. Liu, H. Chen, X. Hou, H. Zhang, J. Han, Y.-G. Jiang, X. Zeng, D. W. Zhang, P. Zhou, *Nature Nanotechnology* **2019**, *14*, 7 662.
- [3] G. Migliato Marega, Y. Zhao, A. Avsar, Z. Wang, M. Tripathi, A. Radenovic, A. Kis, *Nature* **2020**, *587*, 7832 72.
- [4] S. Bertolazzi, D. Krasnozhon, A. Kis, *ACS Nano* **2013**, *7*, 4 3246.
- [5] C. Liu, X. Yan, X. Song, S. Ding, D. W. Zhang, P. Zhou, *Nature Nanotechnology* **2018**, *13*, 5 404.
- [6] V. K. Sangwan, D. Jariwala, I. S. Kim, K.-S. Chen, T. J. Marks, L. J. Lauhon, M. C. Hersam, *Nature Nanotechnology* **2015**, *10*, 5 403.
- [7] R. Ge, X. Wu, M. Kim, J. Shi, S. Sonde, L. Tao, Y. Zhang, J. C. Lee, D. Akinwande, *Nano Letters* **2018**, *18*, 1 434, pMID: 29236504.
- [8] X. Zhang, J. Grajal, J. L. Vazquez-Roy, U. Radhakrishna, X. Wang, W. Chern, L. Zhou, Y. Lin, P.-C. Shen, X. Ji, X. Ling, A. Zubair, Y. Zhang, H. Wang, M. Dubey, J. Kong, M. Dresselhaus, T. Palacios, *Nature* **2019**, *566*, 7744 368.
- [9] C. Liu, H. Chen, S. Wang, Q. Liu, Y.-G. Jiang, D. W. Zhang, M. Liu, P. Zhou, *Nature Nanotechnology* **2020**, *15*, 7 545.



- [10] W. Han, P. Huang, L. Li, F. Wang, P. Luo, K. Liu, X. Zhou, H. Li, X. Zhang, Y. Cui, T. Zhai, *Nature Communications* **2019**, *10*, 1 4728.
- [11] K. Liu, B. Jin, W. Han, X. Chen, P. Gong, L. Huang, Y. Zhao, L. Li, S. Yang, X. Hu, J. Duan, L. Liu, F. Wang, F. Zhuge, T. Zhai, *Nature Electronics* **2021**, *4*, 12 906.
- [12] K. Liu, L. Liu, T. Zhai, *The Journal of Physical Chemistry Letters* **2022**, *13*, 9 2173, pMID: 35230116.
- [13] S. Lebègue, T. Björkman, M. Klintonberg, R. M. Nieminen, O. Eriksson, *Phys. Rev. X* **2013**, *3* 031002.
- [14] G. Cheon, K.-A. N. Duerloo, A. D. Sendek, C. Porter, Y. Chen, E. J. Reed, *Nano Letters* **2017**, *17*, 3 1915, pMID: 28191965.
- [15] N. Mounet, M. Gibertini, P. Schwaller, D. Campi, A. Merkys, A. Marrazzo, T. Sohier, I. E. Castelli, A. Cepellotti, G. Pizzi, N. Marzari, *Nature Nanotechnology* **2018**, *13*, 3 246.
- [16] R. Friedrich, M. Ghorbani-Asl, S. Curtarolo, A. V. Krasheninnikov, *Nano Letters* **2022**, *22*, 3 989, pMID: 35051335.
- [17] A. Jain, S. P. Ong, G. Hautier, W. Chen, W. D. Richards, S. Dacek, S. Cholia, D. Gunter, D. Skinner, G. Ceder, K. a. Persson, *APL Materials* **2013**, *1*, 1 011002.
- [18] P. Gorai, E. S. Toberer, V. Stevanović, *J. Mater. Chem. A* **2016**, *4* 11110.
- [19] P. M. Larsen, M. Pandey, M. Strange, K. W. Jacobsen, *Phys. Rev. Materials* **2019**, *3* 034003.
- [20] W. Storzer, D. Schomburg, G.-V. Rösenthaller, R. Schmutzler, *Chemische Berichte* **1983**, *116*, 1 367.
- [21] J. Rosdahl, M. Gorlov, A. Fischer, L. Kloo, *Zeitschrift für anorganische und allgemeine Chemie* **2004**, *630*, 5 760.
- [22] A. Benrath, B. Schiffers, *Zeitschrift für anorganische und allgemeine Chemie* **1938**, *240*, 1 67.
- [23] H. J. Whitfield, *J. Chem. Soc., Dalton Trans.* **1973**, 1740–1742.
- [24] H.-P. Komsa, A. V. Krasheninnikov, *Phys. Rev. B* **2012**, *86* 241201.
- [25] Y. Lin, X. Ling, L. Yu, S. Huang, A. L. Hsu, Y.-H. Lee, J. Kong, M. S. Dresselhaus, T. Palacios, *Nano Letters* **2014**, *14*, 10 5569, pMID: 25216267.
- [26] A. Chernikov, T. C. Berkelbach, H. M. Hill, A. Rigosi, Y. Li, O. B. Aslan, D. R. Reichman, M. S. Hybertsen, T. F. Heinz, *Phys. Rev. Lett.* **2014**, *113* 076802.
- [27] M. M. Ugeda, A. J. Bradley, S.-F. Shi, F. H. da Jornada, Y. Zhang, D. Y. Qiu, W. Ruan, S.-K. Mo, Z. Hussain, Z.-X. Shen, F. Wang, S. G. Louie, M. F. Crommie, *Nature Materials* **2014**, *13*, 12 1091.
- [28] K. Waizumi, H. Masuda, H. Ohtaki, *Inorganica Chimica Acta* **1992**, *192*, 2 173.
- [29] P. Clare, T. J. King, D. B. Sowerby, *J. Chem. Soc., Dalton Trans.* **1974**, 2071–2074.
- [30] A. B. Venediktov, S. V. Korenev, D. B. Vasil'chenko, A. V. Zadesenets, E. Y. Filatov, S. N. Mamonov, L. V. Ivanova, N. G. Prudnikova, E. Y. Semitut, *Russian Journal of Applied Chemistry* **2012**, *85*, 7 995.
- [31] B. Krebs, C. Brendel, H. Schäfer, *Zeitschrift für anorganische und allgemeine Chemie* **1988**, *561*, 1 119.
- [32] T. Björkman, A. Gulans, A. V. Krasheninnikov, R. M. Nieminen, *Phys. Rev. Lett.* **2012**, *108* 235502.

- [33] T. Björkman, *The Journal of Chemical Physics* **2014**, *141*, 7 074708.
- [34] C. Chakraborty, L. Kinnischtzke, K. M. Goodfellow, R. Beams, A. N. Vamivakas, *Nature Nanotechnology* **2015**, *10*, 6 507.
- [35] M. Toth, I. Aharonovich, *Annual Review of Physical Chemistry* **2019**, *70*, 1 123, PMID: 30735459.
- [36] P. Kumar, J. Lynch, B. Song, H. Ling, F. Barrera, K. Kisslinger, H. Zhang, S. B. Anantharaman, J. Digani, H. Zhu, T. H. Choudhury, C. McAleese, X. Wang, B. R. Conran, O. Whear, M. J. Motala, M. Snure, C. Muratore, J. M. Redwing, N. R. Glavin, E. A. Stach, A. R. Davoyan, D. Jariwala, *Nature Nanotechnology* **2022**, *17*, 2 182.
- [37] C. Wang, Q. He, U. Halim, Y. Liu, E. Zhu, Z. Lin, H. Xiao, X. Duan, Z. Feng, R. Cheng, N. O. Weiss, G. Ye, Y.-C. Huang, H. Wu, H.-C. Cheng, I. Shakir, L. Liao, X. Chen, W. A. Goddard III, Y. Huang, X. Duan, *Nature* **2018**, *555* 231.
- [38] Y.-C. Lin, A. Motoyama, S. Kretschmer, S. Ghaderzadeh, M. Ghorbani-Asl, Y. Araki, A. V. Krashennnikov, H. Ago, K. Suenaga, *Advanced Materials* **2021**, *33*, 52 2105898.
- [39] X. Feng, Z. Sun, K. Pei, W. Han, F. Wang, P. Luo, J. Su, N. Zuo, G. Liu, H. Li, T. Zhai, *Advanced Materials* **2020**, *32*, 32 2003146.
- [40] S. P. Ong, S. Cholia, A. Jain, M. Brafman, D. Gunter, G. Ceder, K. A. Persson, *Computational Materials Science* **2015**, *97* 209.
- [41] A. H. Larsen, J. J. Mortensen, J. Blomqvist, I. E. Castelli, R. Christensen, M. Dulak, J. Friis, M. N. Groves, B. Hammer, C. Hargus, E. D. Hermes, P. C. Jennings, P. B. Jensen, J. Kermode, J. R. Kitchin, E. L. Kolsbjerg, J. Kubal, K. Kaasbjerg, S. Lysgaard, J. B. Maronsson, T. Maxson, T. Olsen, L. Pastewka, A. Peterson, C. Rostgaard, J. Schiøtz, O. Schütt, M. Strange, K. S. Thygesen, T. Vegge, L. Vilhelmsen, M. Walter, Z. Zeng, K. W. Jacobsen, *Journal of Physics: Condensed Matter* **2017**, *29*, 27 273002.
- [42] A. Hagberg, P. Swart, D. S Chult, Exploring network structure, dynamics, and function using networkx, Technical report, Los Alamos National Lab.(LANL), Los Alamos, NM (United States), **2008**.
- [43] G. Kresse, J. Furthmüller, *Phys. Rev. B* **1996**, *54* 11169.
- [44] G. Kresse, D. Joubert, *Phys. Rev. B* **1999**, *59* 1758.
- [45] I. Hamada, *Phys. Rev. B* **2014**, *89* 121103.
- [46] M. Dion, H. Rydberg, E. Schröder, D. C. Langreth, B. I. Lundqvist, *Phys. Rev. Lett.* **2004**, *92* 246401.
- [47] G. Román-Pérez, J. M. Soler, *Phys. Rev. Lett.* **2009**, *103* 096102.
- [48] J. c. v. Klimeš, D. R. Bowler, A. Michaelides, *Phys. Rev. B* **2011**, *83* 195131.
- [49] P. V. C. Medeiros, S. Stafström, J. Björk, *Phys. Rev. B* **2014**, *89* 041407.

# Screening 0D materials for 2D nanoelectronics applications

Mohammad Bagheri and Hannu-Pekka Komsa

<sup>1</sup>*Microelectronics Research Unit, University of Oulu, Oulu, Finland*

(Dated: March 15, 2022)

## I. TABLES

TABLE I: List of of all 162 materials found from the MP database search. Formula, MP-ID,  $E_{\text{hull}}$  (in eV),  $E_g$  (in eV), and  $\epsilon_0$  are extracted from MP. Cluster formula are cleaned up to match the notation used in literature and not reduced to indicate the actual number of atoms in the cluster. Names are extracted from literature. Asterisk refers to materials that were determined to be metastable. Melting point (mp.) and boiling point (bp.) are extracted from literature, as indicated by the source. The corresponding Wikipedia entry can be found using the name.

Name	Formula	Cluster	MP-ID	$E_{\text{hull}}$	$E_g$	$\epsilon_0$	mp.	bp.	source
aluminum borohydride	Al(BH4)3	Al(BH4)3	mp-569787	0.0	6.24	3.40	-64.5	44.5	Wikipedia
	Al2PdCl8	Al2Cl8Pd	mp-27452	0.0	1.68	3.51			[1]
aluminium iodide	AlI3	Al2I6	mp-30930	0.0	3.27	3.73	188.3	382.0	Wikipedia
	AlSCl3O2	[Cl2Al(mu-O2SCl)]2	mp-556418	0.0	3.98	3.51	0.0		[2]
arsenic trioxide (cubic)	As2O3	As4O6	mp-2184	0.009	4.03	3.83	312.2	465.0	Wikipedia
uzonite	As4S5	As4S5	mp-502	0.003	2.01	5.45			[3]
arsenic trichloride	AsCl3	AsCl3	mp-23280	0.0	4.10	3.33	-16.2	130.2	Wikipedia
	AsCl3O	(AsOCl3)2	mp-29863	0.0	2.54	3.13	0.0		[4]
arsenic pentachloride	AsCl5	AsCl5	mp-30106	0.0	1.46	3.07	-50.0		Wikipedia
arsenic trifluoride	AsF3	AsF3	mp-28027	0.0	5.40	5.24	-8.5	60.4	Wikipedia
arsenic pentafluoride	AsF5	AsF5	mp-8723	0.0	4.63	2.35	-79.8	-52.8	Wikipedia
realgar	AsS	As4S4	mp-542846	0.004	2.05	4.85	320.0		Wikipedia
gold chloride	AuCl3	Au2Cl6	mp-27647	0.0	1.39	3.93	254.0		Wikipedia
boric acid	B(OH)3	B(OH)3	mp-759069	0.003	6.09	2.81	170.9	300.0	Wikipedia
*	B3H5	B6H10	mp-29721	0.038	3.88	2.85	-62.3	108.0	[5]
	BBr	B9Br9	mp-685043	0.009	1.43	3.71			[6]
boron tribromide	BBr3	BBr3	mp-23225	0.0	3.87	2.37	-46.3	91.3	Wikipedia
boron trichloride	BCl3	BCl3	mp-23184	0.0	4.75	2.20	-107.3	12.6	Wikipedia
boron trifluoride	BF3	BF3	mp-558149	0.0	8.16	2.19	-126.8	-100.3	Wikipedia
* H2O-BF3 adduct	BH2OF3	H2OBF3	mp-707009	0.0	7.57	3.54			Wikipedia
ammonia borane	BH6N	BNH6	mp-35082	0.001	6.07	5.19	104.0		Wikipedia
*	BH6N	BNH6	mp-675418	0.012	5.89	9.14			-
boron triiodide	BI3	BI3	mp-23189	0.0	0.00	2.94	49.9	210.0	Wikipedia
dibromine trioxide	Br2O3	Br2O3	mp-28933	0.0	1.79	7.16	-40.0		Wikipedia
bromine pentafluoride	BrF5	BrF5	mp-27987	0.0	3.46	3.16	-61.3	40.2	Wikipedia
bromyl fluoride	BrO2F	BrFO2	mp-36262	0.0	2.90	3.68	-9.0	55.0	[7]
dichlorodifluoromethane	C(ClF)2	CCl2F2	mp-22966	0.015	5.74	2.43	-157.7	-29.8	Wikipedia
trichlorofluoromethane	CCl3F	CCl3F	mp-23071	0.012	4.90	3.15	-110.5	23.8	Wikipedia
chlorotrifluoromethane	CClF3	CClF3	mp-28473	0.012	6.72	31.05	-181.0	-81.5	Wikipedia
tetrafluoromethane	CF4	CF4	mp-1167	0.0	9.07	1.93	-183.6	-127.8	Wikipedia
cyanuric chloride	CNCl	(NCCl)3	mp-571324	0.0	3.79	2.78	144.0	192.0	Wikipedia
dichlorine heptoxide	Cl2O7	Cl2O7	mp-31050	0.0	3.68	3.14	-91.6	82.0	Wikipedia
chlorine trifluoride	ClF3	ClF3	mp-556767	0.005	2.63	3.52	-76.3	11.8	Wikipedia
CoBr2.4H2O	CoH8(BrO2)2	CoBr2(H2O)4	mp-23965	0.053	2.20	5.03			[8, 9]
* chromium hexafluoride	CrF6	CrF6	mp-1539213	0.0	2.09	3.21			Wikipedia
FeBr2.4H2O	FeH8(BrO2)2	FeBr2(H2O)4	mp-24537	0.026	3.72	4.96			[9]
gallium bromide	GaBr3	Ga2Br6	mp-30953	0.0	3.36	3.37	121.5	278.8	Wikipedia
gallium trichloride	GaCl3	Ga2Cl6	mp-30952	0.0	4.28	3.36	77.9	201.0	Wikipedia
Hg2(GaCl4)2	GaHgCl4	Hg2(GaCl4)2	mp-1103091	0.0	2.86	7.45			[10]
germanium tetrachloride	GeCl4	GeCl4	mp-30086	0.0	4.27	2.56	-49.5	86.5	Wikipedia
germanium tetrafluoride	GeF4	GeF4	mp-9816	0.0	5.68	2.69	-15.0	-36.5	Wikipedia
germyl chloride	GeH3Cl	GeH3Cl	mp-28369	0.0	4.76	3.78	0.0		[11]

hydrogen peroxide	H2O2	H2O2	mp-28015	0.082	4.51	3.95	-0.4	150.2	Wikipedia
sulfuric acid	H2SO4	H2SO4	mp-625475	0.0	6.09	3.77	10.3	337.0	Wikipedia
*	H2SO4	H2SO4	mp-690733	0.000	6.11	3.59			-
*	H2SO4	H2SO4	mp-24172	0.004	6.05	3.86			-
selenous acid	H2SeO3	H2SeO3	mp-27996	0.003	4.50	5.83	70.0		Wikipedia
selenic acid	H2SeO4	H2SeO4	mp-23866	0.0	3.42	4.81	58.0	260.0	Wikipedia
ammonia	H3N	H3N	mp-29145	0.0	4.34	2.99	-77.7	-33.3	Wikipedia
*	H3N	H3N	mp-643432	0.017	4.46	3.52			-
*	H3N	H3N	mp-779689	0.022	3.75	3.26			-
methane	H4C	CH4	mp-1021328	0.0	7.64	1.66	-182.5	-161.5	Wikipedia
urea	H4CN2O	CH4N2O	mp-23778	0.0	5.08	3.80	133.0		Wikipedia
*	H4CN2O	CH4N2O	mp-976707	0.023	5.05	4.65			-
thiourea	H4CSN2	CH4N2S	mp-721896	0.006	3.33	7.41	182.0		Wikipedia
*	H4CSN2	CH4N2S	mp-634059	0.054	2.84	5.54			-
platinic acid	H8PtO6	H2Pt(OH)6	mp-625112	0.069	1.59	40.58			[12]
*	H8PtO6	H2Pt(OH)6	mp-625111	0.070	1.60	11.82			-
*	H8PtO6	H2Pt(OH)6	mp-625113	0.084	1.52	9.37			-
iodic acid	HIO3	HIO3	mp-556216	0.018	3.07	8.64	110.0		Wikipedia
	HS8N	HNS8	mp-29491	0.014	2.61	3.59	85.0		[13]
mercury bromide	HgBr	Hg2Br2	mp-23177	0.0	2.46	25.24	405.0	390.0	Wikipedia
mercury chloride	HgCl	Hg2Cl2	mp-22897	0.0	2.82	17.40	276.0	304.0	Wikipedia
iodine trichloride	ICl3	I2Cl6	mp-27729	0.0	1.81	4.71	63.0		Wikipedia
iodine heptafluoride	IF7	IF7	mp-27988	0.0	1.55	2.50	4.5	4.8	Wikipedia
	LiS4	Li2S8	mp-995393	0.0	2.16	1.27			No expt data found
magnesium perchlorate	MgH8(ClO6)2	Mg(ClO4)2(H2O)4	mp-865188	0.0	5.33	4.79	251.0		Wikipedia
*	MgH8(ClO6)2	Mg(ClO4)2(H2O)4	mp-989229	0.009	5.22	4.98			-
molybdenum hexafluoride	MoF6	MoF6	mp-558836	0.005	4.25	2.55	17.5	34.0	Wikipedia
chlorine nitrate	NCIO3	CINO3	mp-754712	0.0	2.94	3.10	-107.0	18.0	[14]
nitric oxide	NO2	N2O4	mp-557865	0.020	2.87	2.29	-151.8	-151.8	[15]
	NbAlCl8	AlCl8Nb	mp-28358	0.0	2.02	3.69	139.7		[16]
niobium iodide	NbI5	Nb2I10	mp-569578	0.0	0.99	8.83	543.0		Wikipedia
osmium tetroxide	OsO4	OsO4	mp-540783	0.0	3.30	2.57	40.2	129.7	Wikipedia
*	OsO4	OsO4	mp-551905	0.001	3.29	2.65			-
osmium oxide pentafluoride	OsOF5	F5Oos	mp-555514	0.000	0.81	3.42	32.5		[17]
phosphorus pentoxide	P2O5	P4O10	mp-562613	0.010	5.55	2.88	340.0	360.0	Wikipedia
phosphorus sulfoxide	P2S2O3	P4S4O6	mp-3667	0.0	4.01	3.13	102.0	295.0	[18]
Pt(PF3)4	P4PtF12	Pt(PF3)4	mp-555863	0.0	4.99	2.91	-15.0	86.0	[19]
phosphorus sulfide	P4S5	P4S5	mp-690	0.004	2.49	4.32	288.0	514.0	Wikipedia
phosphorus selenide	P4Se5	P4Se5	mp-2447	0.018	1.83	6.80			Wikipedia
phosphorus tribromide	PBr3	Br3P	mp-27257	0.0	3.35	3.03	-41.5	173.2	Wikipedia
phosphorus oxybromide	PBr3O	Br3OP	mp-558645	0.0	3.33	4.04	56.0	189.5	[20]
	PBrNF	P3N3Br3F3	mp-559366	0.014	4.25	3.08			[21]
phosphorus trichloride	PCl3	PCl3	mp-23230	0.0	4.08	2.77	-93.6	76.1	Wikipedia
phosphoryl chloride	POCl3	POCl3	mp-27277	0.0	4.68	3.29	1.2	105.8	Wikipedia
*	POCl3	POCl3	mp-753611	0.006	4.56	3.52			-
phosphoryl chloride difluoride	PClOF2	ClF2OP	mp-558681	0.0	5.73	2.88	-96.4	3.1	Wikipedia
phosphorus pentafluoride	PF5	PF5	mp-8511	0.0	7.11	2.15	-93.8	-84.6	Wikipedia
fluorophosphorane	PH2F3	PH2F3	mp-29515	0.0	6.47	12.44	-47.0	0.9	[22]
	PH3CS3	(CH3S)2(P2S2)S2	mp-559616	0.021	2.18	4.21			[23]
NH3-PF5 adduct	PH3NF5	NH3PF5	mp-722832	0.0	7.09	6.27			[24]
phosphoric acid	PH3O4	H3PO4	mp-23902	0.0	6.23	4.76	40.0	212.0	Wikipedia
*	PH3O4	H3PO4	mp-626449	0.011	5.81	5.91			-
*	PH3O4	H3PO4	mp-626464	0.023	5.65	5.53			-
	PHF4	PHF4	mp-29514	0.0	7.55	2.59	-80.0	-39.0	[25]
hydrophosphoryl difluoride	PHOF2	OPF2H	mp-698060	0.011	7.00	3.22	55.0	55.0	[26]
hydrothiophosphoryl difluoride	PHSF2	SPF2H	mp-642795	0.0	4.57	3.14	0.2	0.2	[26]
phosphorus iodide	PI2	P2I4	mp-29443	0.0	2.06	4.25	125.5		Wikipedia
phosphorus iodide	PI3	PI3	mp-27529	0.0	2.36	4.11	61.2	200.0	Wikipedia
hexachlorophosphazene	PNCI2	(NPCl2)3	mp-571213	0.000	3.85	3.24	112.0		Wikipedia
	PNCIF	P3N3Cl3F3	mp-554472	0.008	5.08	2.89			[21]
(PNF2)4	PNF2	F8N4P4	mp-555292	0.004	5.17	3.28	28.0	89.7	[27]
	Pd(SCl3)2	PdS2Cl6	mp-28174	0.0	1.62	5.32			[28]
	Pd(SeCl3)2	PdSe2Cl6	mp-28175	0.0	1.72	4.67			[29]
palladium chloride	PdCl2	Pd6Cl12	mp-29487	0.0	1.43	3.96	679.0		Wikipedia

platinum chloride	PtCl <sub>2</sub>	Pt6Cl <sub>12</sub>	mp-23290	0.0	1.83	3.29	581.0		Wikipedia
perrhenic acid	Re <sub>2</sub> H <sub>4</sub> O <sub>9</sub>	Re <sub>2</sub> O <sub>7</sub> (OH <sub>2</sub> ) <sub>2</sub>	mp-625238	0.026	2.64	11.38	115.0		[30]
*	Re <sub>2</sub> O <sub>7</sub>	Re <sub>2</sub> O <sub>7</sub>	mvc-7040	0.039	3.47	3.19			-
ruthenium tetroxide	RuO <sub>4</sub>	RuO <sub>4</sub>	mp-554791	0.0	2.43	2.77	25.4	40.0	Wikipedia
	RuS <sub>3</sub> Cl <sub>8</sub>	Ru <sub>2</sub> S <sub>6</sub> Cl <sub>16</sub>	mp-29568	0.0	1.90	5.24	122.0		[31]
sulfur (alpha)	S	S <sub>8</sub>	mp-77	0.001	2.71	2.95	115.2	444.6	Wikipedia
*	S	S <sub>12</sub>	mp-558014	0.014	2.48	3.09			-
*	S	S <sub>14</sub>	mp-561513	0.019	2.43	3.44			-
sulfuryl chloride	S(ClO) <sub>2</sub>	SO <sub>2</sub> Cl <sub>2</sub>	mp-28405	0.0	3.79	3.46	-54.1	69.4	Wikipedia
sulfuryl trifluoride	S(OF) <sub>2</sub>	SO <sub>2</sub> F <sub>2</sub>	mp-8537	0.0	5.90	2.33	-124.7	-55.4	Wikipedia
disulfuryl difluoride	S <sub>2</sub> O <sub>5</sub> F <sub>2</sub>	S <sub>2</sub> O <sub>5</sub> F <sub>2</sub>	mp-28676	0.0	5.61	2.75	-48.1	50.9	[32]
disulfur dibromide	SBr	Br <sub>2</sub> S <sub>2</sub>	mp-28099	0.0	2.31	5.41	46.0	46.0	Wikipedia
thionyl bromide	SBr <sub>2</sub> O	Br <sub>2</sub> OS	mp-28407	0.0	2.73	3.57	0.0		[33]
disulfur dichloride	SCl	S <sub>2</sub> Cl <sub>2</sub>	mp-28096	0.0	2.89	3.22	-80.0	137.1	Wikipedia
thionyl chloride	SCl <sub>2</sub> O	SOCl <sub>2</sub>	mp-28406	0.0	3.64	3.05	-104.5	74.6	Wikipedia
sulfuryl chloride fluoride	SClO <sub>2</sub> F	SO <sub>2</sub> ClF	mp-554012	0.0	4.68	2.79	-124.7	7.1	Wikipedia
sulfur hexafluoride	SF <sub>6</sub>	SF <sub>6</sub>	mp-8560	0.0	5.91	2.15	-64.0	-50.8	Wikipedia
*	SF <sub>6</sub>	SF <sub>6</sub>	mp-975	0.001	5.92	2.38			-
sulfur trioxide	SO <sub>3</sub>	S <sub>3</sub> O <sub>9</sub>	mp-2414	0.0	5.14	2.78	16.9	45.0	Wikipedia
antimony trioxide	Sb <sub>2</sub> O <sub>3</sub>	Sb <sub>4</sub> O <sub>6</sub>	mp-1999	0.008	3.41	8.42	656.0	1425.0	Wikipedia
antimony tribromide	SbBr <sub>3</sub>	Br <sub>3</sub> Sb	mp-27399	0.0	3.45	4.00	96.6	288.0	Wikipedia
antimony trichloride	SbCl <sub>3</sub>	SbCl <sub>3</sub>	mp-22872	0.0	3.75	7.67	73.4	223.5	Wikipedia
	SbCl <sub>3</sub> F <sub>2</sub>	(SbCl <sub>3</sub> F <sub>2</sub> ) <sub>4</sub>	mp-560748	0.004	1.71	4.47	62.0		[34]
selenium (beta)	Se	Se <sub>8</sub>	mp-542605	0.006	1.40	5.33	221.0	685.0	Wikipedia
diselenidibromid	SeBr	Br <sub>2</sub> Se <sub>2</sub>	mp-570589	0.006	1.55	6.31	-49.0	225.0	[35]
selenium tetrafluoride	SeF <sub>4</sub>	SeF <sub>4</sub>	mp-29172	0.0	4.14	6.68	-13.2	101.0	Wikipedia
seleninyl difluoride	SeOF <sub>2</sub>	F <sub>2</sub> OSe	mp-27367	0.0	4.10	4.18	15.0		[36]
	Si <sub>2</sub> Cl <sub>2</sub> O <sub>3</sub>	Cl <sub>8</sub> Si <sub>8</sub> O <sub>12</sub>	mp-28959	0.026	5.68	2.94			[37]
octahydridosilsesquioxane	Si <sub>2</sub> H <sub>2</sub> O <sub>3</sub>	Si <sub>8</sub> H <sub>8</sub> O <sub>12</sub>	mp-24431	0.023	6.37	3.23			[38]
	Si <sub>2</sub> H <sub>2</sub> S <sub>3</sub>	Si <sub>4</sub> H <sub>4</sub> S <sub>6</sub>	mp-28090	0.0	3.37	3.62			[39]
disiloxane	Si <sub>2</sub> H <sub>6</sub> O	Si <sub>2</sub> H <sub>6</sub> O	mp-27949	0.050	5.26	2.86	-15.2	-15.2	Wikipedia
disilyl selenide	Si <sub>2</sub> H <sub>6</sub> Se	Si <sub>2</sub> H <sub>6</sub> Se	mp-29310	0.000	3.75	3.62	-68.0	85.0	[40]
silicon tetrabromide	SiBr <sub>4</sub>	SiBr <sub>4</sub>	mp-570285	0.0	4.11	2.61	5.0	153.0	Wikipedia
cyclic chlorosiloxane	SiCl <sub>2</sub> O	(SiCl <sub>2</sub> O) <sub>4</sub>	mp-23079	0.015	5.57	2.81	77.0		[41]
cyclic chlorosiloxane	SiCl <sub>2</sub> O	(SiCl <sub>2</sub> O) <sub>3</sub>	mp-23563	0.027	5.57	2.64	43.5		[41]
silicon tetrachloride	SiCl <sub>4</sub>	SiCl <sub>4</sub>	mp-28391	0.0	5.79	2.40	-68.7	57.6	Wikipedia
silicon tetrafluoride	SiF <sub>4</sub>	SiF <sub>4</sub>	mp-1818	0.0	7.94	2.16	-95.0	-90.3	Wikipedia
silyl fluoride	SiH <sub>3</sub> F	SiH <sub>3</sub> F	mp-28289	0.024	6.01	2.62	-98.6	-98.6	[42]
iodosilane	SiH <sub>3</sub> I	SiH <sub>3</sub> I	mp-28538	0.0	4.21	3.70	-57.0	45.4	[43]
silane	SiH <sub>4</sub>	SiH <sub>4</sub>	mp-23739	0.005	6.59	2.47	-185.0	-111.9	Wikipedia
SiF <sub>4</sub> -2NH <sub>3</sub> adduct	SiH <sub>6</sub> (NF <sub>2</sub> ) <sub>2</sub>	SiF <sub>4</sub> (NH <sub>3</sub> ) <sub>2</sub>	mp-643277	0.0	6.70	3.21	166.0		[44]
tin iodide	SnI <sub>4</sub>	SnI <sub>4</sub>	mp-571436	0.019	1.78	3.40	143.0	348.5	Wikipedia
	Ta <sub>4</sub> S <sub>9</sub> Br <sub>8</sub>	Ta <sub>4</sub> S <sub>9</sub> Br <sub>8</sub>	mp-559724	0.0	1.30	4.38			[45]
	TaCl <sub>4</sub> F	(TaCl <sub>4</sub> F) <sub>4</sub>	mp-27854	0.0	3.10	4.44			[46]
telluric acid	Te(OH) <sub>6</sub>	Te(OH) <sub>6</sub>	mp-626012	0.050	2.23	5.28	136.0		Wikipedia
*	Te(OH) <sub>6</sub>	Te(OH) <sub>6</sub>	mp-625993	0.060	2.00	5.40			-
trioxotetrafluoroditelluric acid	Te <sub>2</sub> H <sub>2</sub> O <sub>3</sub> F <sub>4</sub>	H <sub>2</sub> Te <sub>2</sub> O <sub>3</sub> F <sub>4</sub>	mp-1191341	0.0	4.62	7.89			[47]
tellurium hexafluoride	TeF <sub>6</sub>	TeF <sub>6</sub>	mp-1875	0.0	4.40	2.47	-38.9	-37.6	Wikipedia
*	TeF <sub>6</sub>	TeF <sub>6</sub>	mp-1542727	0.001	4.44	2.44			-
	TeS <sub>7</sub> Br <sub>2</sub>	Br <sub>2</sub> S <sub>7</sub> Te	mp-683875	0.003	2.23	4.12			[48]
	TeS <sub>7</sub> Cl <sub>2</sub>	Cl <sub>2</sub> S <sub>7</sub> Te	mp-672186	0.0	2.26	4.43			[48]
titanium tetrabromide	TiBr <sub>4</sub>	TiBr <sub>4</sub>	mp-569814	0.0	2.84	2.78	39.0	230.0	Wikipedia
titanium tetrachloride	TiCl <sub>4</sub>	TiCl <sub>4</sub>	mp-30092	0.0	3.47	2.52	-24.1	136.4	Wikipedia
tungsten hexachloride	WCl <sub>6</sub>	WCl <sub>6</sub>	mp-571518	0.0	1.92	4.94	275.0	346.7	Wikipedia
*	WCl <sub>6</sub>	WCl <sub>6</sub>	mp-23178	0.000	1.75	4.45			-
xenon tetrafluoride	XeF <sub>4</sub>	XeF <sub>4</sub>	mp-23185	0.0	2.86	3.48	117.0		Wikipedia

TABLE II: Additional materials found by graph-theoretical approach. All information is as in Table S1.

Name	Formula	Cluster	MP-ID	$E_{\text{hull}}$	$E_g$	$\epsilon_0$	mp.	bp.	source
* bismuth oxide	Bi <sub>2</sub> O <sub>3</sub>	Bi <sub>4</sub> O <sub>6</sub>	mp-1188267	0.072	2.60				Wikipedia
* nitrogen	N <sub>2</sub>	N <sub>10</sub>	mp-1080711	0.0	0.00				[49]

phosphorus trioxide	P2O3	P4O6	mp-368	0.088	3.85	23.8	173.1	Wikipedia
P4S5 (beta)	P4S5	P4S5	mp-7260	0.017	2.61	103.0		[50]
arsenic selenide	AsSe	As4Se4	mp-542570	0.005	1.54	265.0		[51]
P4S4 (alpha)	PS	P4S4	mp-612	0.020	2.52	134.0		[50]
germanium thiobromide	Ge2S3Br2	Ge4S6Br4	mp-540792	0.0	2.46	305.0		[52]
germanium thioiodide	Ge2S3I2	Ge4S6I4	mp-27928	0.0	2.25	310.0		[52]
phosphorus pentasulfide	P2S5	P4S10	mp-541788	0.0	2.58	288.0	514.0	Wikipedia
niobium bromide	NbBr5	Nb2Br10	mp-28601	0.0	1.56	254.0	364.0	Wikipedia
*	NbBr5	Nb2Br10	mp-568245	0.004	1.60			-
tantalum bromide	TaBr5	Ta2Br10	mp-1203015	0.0	2.03	265.0	349.0	Wikipedia
*	TaBr5	Ta2Br10	mp-568846	0.000	2.03			-
tungsten bromide	WBr5	W2Br10	mp-29554	0.012	0.00	286.0	333.0	Wikipedia
*	WBr5	W2Br10	mp-1095321	0.012	0.00			-
molybdenum chloride	MoCl5	Mo2Cl10	mp-569855	0.0	0.00	194.0	268.0	Wikipedia
*	MoCl5	Mo2Cl10	mp-569436	0.003	0.00			-
*	MoCl5	Mo2Cl10	mp-571256	0.003	0.00			-
*	MoCl5	Mo2Cl10	mp-29147	0.019	0.00			-
niobium chloride	NbCl5	Nb2Cl10	mp-23307	0.0	2.22	204.7	248.2	Wikipedia
*	NbCl5	Nb2Cl10	mp-568483	0.001	2.30			-
rhenium chloride	ReCl5	Re2Cl10	mp-27645	0.054	0.00	220.0		Wikipedia
antimony chloride	SbCl5	Sb2Cl10	mp-570796	0.003	1.85	-54.1		[53]
vanadium chloride	VCl5	V2Cl10	mp-1101909	0.0	1.05	-10.0		[54]
tungsten chloride	WCl5	W2Cl10	mp-27160	0.022	0.00	248.0	275.6	Wikipedia
rhenium trichloride dioxide	ReCl3O2	Re2O4Cl6	mp-607436	0.0	1.87	35.0		[55]
tantalum iodide	TaI5	Ta2I10	mp-570679	0.0	1.17	382.0		Wikipedia

TABLE III: Additional properties calculated using vdW-DF functional: Cluster formula, MP-ID, binding energy per cluster (eV), volume per cluster ( $\text{\AA}^3$ ), HOMO and LUMO levels of cluster aligned w.r.t. vacuum level (eV), and dipole ( $e\text{\AA}$ ).

formula	MP-ID	binding energy	volume	HOMO	LUMO	dipole
Sb4O6	mp-1999	-4.52	170.94	2.92	4.09	0.01
As4S5	mp-502	-3.31	222.33	1.42	2.64	0.13
As4S4	mp-542846	-2.82	195.84	1.38	2.80	0.00
As4O6	mp-2184	-2.63	162.33	4.04	4.49	0.00
P4O10	mp-562613	-2.17	193.75	5.47	6.01	0.00
Pt6Cl12	mp-23290	-1.69	427.50	1.48	2.01	0.00
Pd6Cl12	mp-29487	-1.75	415.68	1.09	1.64	0.00
Nb2I10	mp-569578	-2.30	454.88	0.61	1.08	0.00
As4Se4	mp-542570	-6.78	208.38	0.85	2.17	0.00
P4S10	mp-541788	-2.94	346.68	2.17	2.97	0.00
Ge4S6Br4	mp-540792	-2.95	387.29	2.14	2.79	0.01
Ge4S6I4	mp-27928	-3.15	455.05	2.06	2.59	0.02
Nb2Br10	mp-28601	-6.58	368.70	1.37	1.70	0.00
Ta2Br10	mp-1203015	-4.74	372.00	1.86	2.19	0.00
Nb2Cl10	mp-23307	-3.87	315.41	2.07	2.33	0.00
Ta2I10	mp-570679	-8.72	459.17	0.94	1.41	0.00

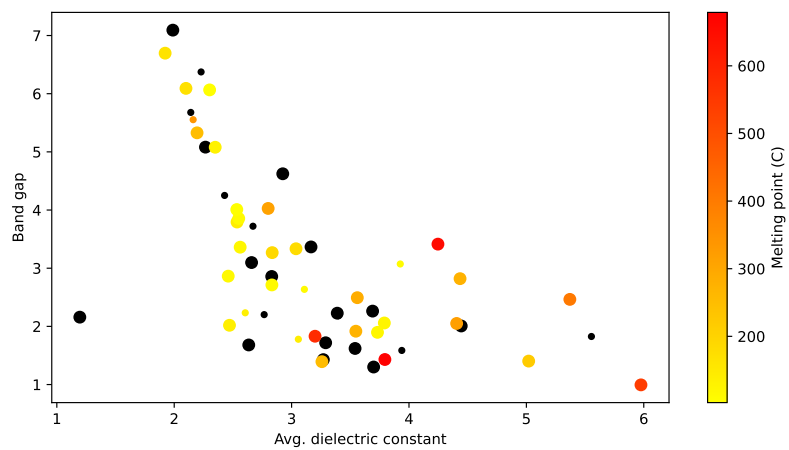


FIG. 1: Band gap vs. high-frequency dielectric constant  $\epsilon_{\infty}$ . Otherwise the same as Figure 1(b) in the main paper.

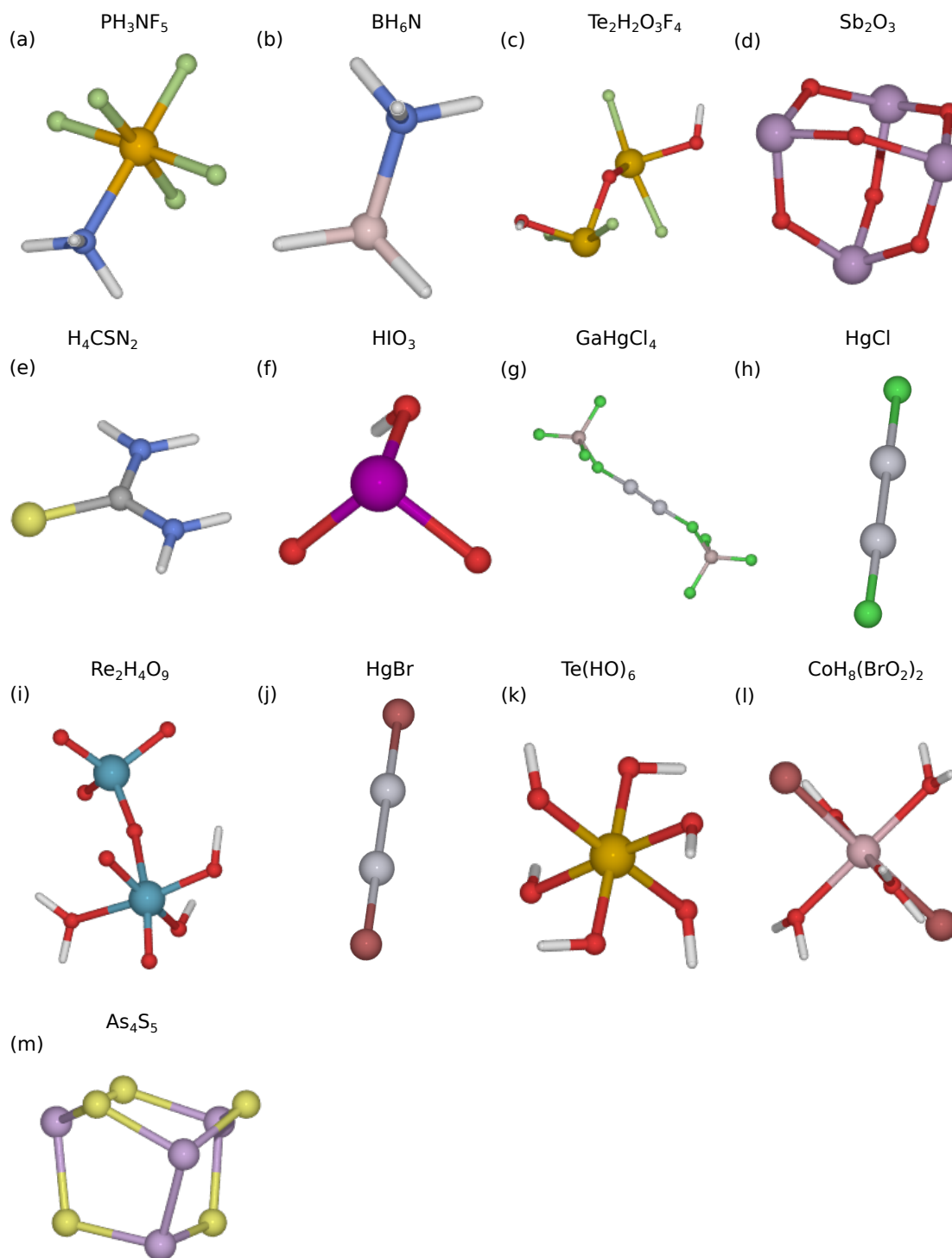


FIG. 2: Atomic structures for all materials included in Figure 1(c) of the main paper.



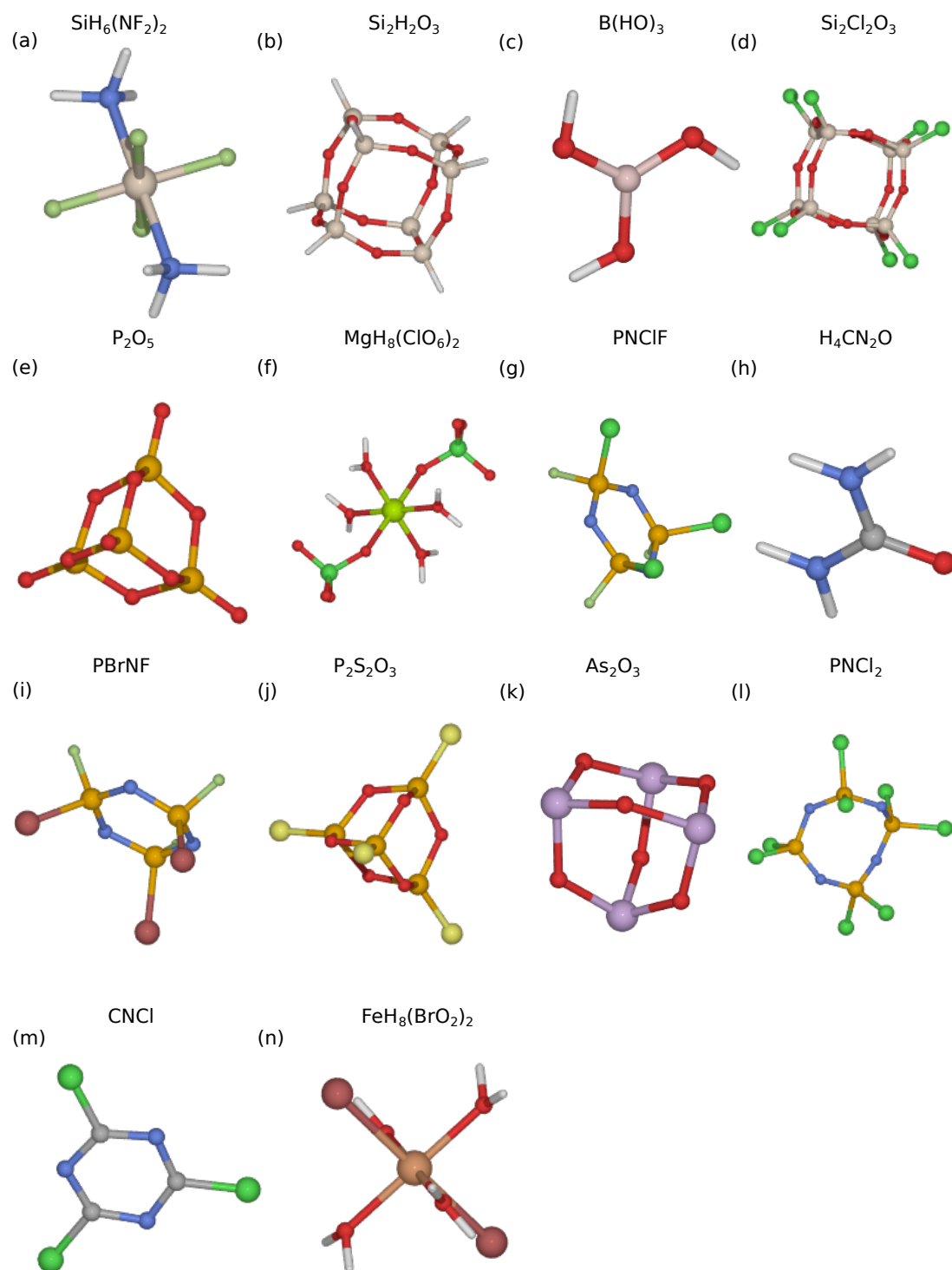


FIG. 3: Atomic structures for all materials included in Figure 1(d) of the main paper.

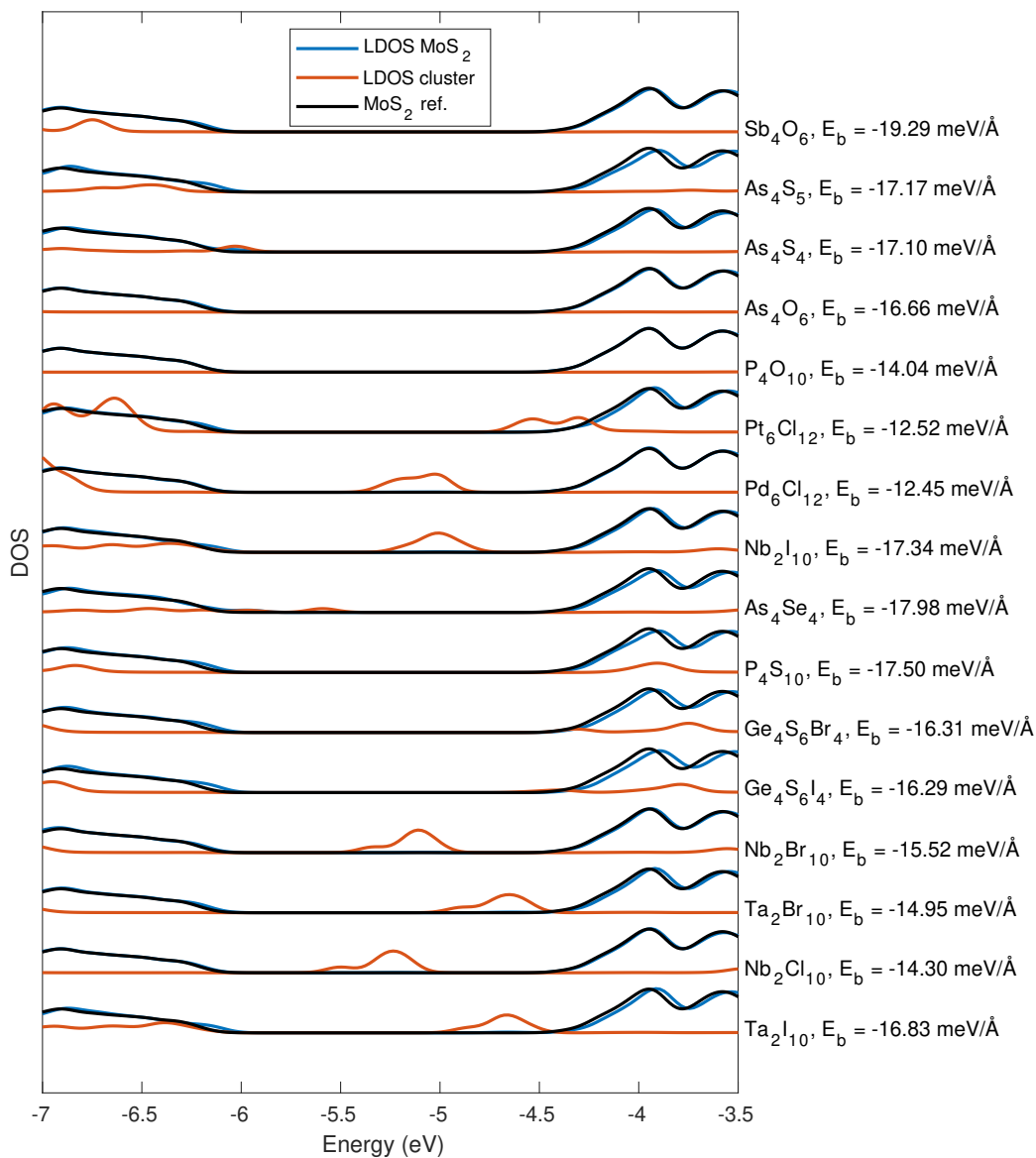


FIG. 4: Electronic structure of 0D clusters adsorbed on MoS<sub>2</sub>. Local density of states of the cluster and of MoS<sub>2</sub> layer. Total DOS pristine MoS<sub>2</sub> is given as a reference. All DOS are aligned using the vacuum level.

- 
- [1] Werner Lenhard, Harald Schäfer, Hans-Ulrich Hürter, and Bernt Krebs. Ein Beitrag zu den Koordinationsverhältnissen in den gasförmigen  $\text{MnCl}_2$ -Komplexen das Spektrum von  $\text{CoCl}_2 \cdot n\text{H}_2\text{O}$  und die Kristallstruktur von  $\text{PdCl}_2$ . *Zeitschrift für anorganische und allgemeine Chemie*, 482(11):19–26, 1981.
- [2] Timothy J. Boyle, Nicholas L. Andrews, Todd M. Alam, David R. Tallant, Mark A. Rodriguez, and David Ingersoll. Speciation in the  $\text{AlCl}_3/\text{SO}_2\text{Cl}_2$  catholyte system. *Inorganic Chemistry*, 44(16):5934–5940, 2005.
- [3] Harold J. Whitfield. Crystal and molecular structure of tetra-arsenic pentasulphide. *J. Chem. Soc., Dalton Trans.*, pages 1740–1742, 1973.
- [4] Silvia Haupt and Konrad Seppelt. The arsenic oxide trichloride dimer. *Zeitschrift für anorganische und allgemeine Chemie*, 626(8):1778–1782, 2000.
- [5] <https://chemdb.net/en/compound/7JyenbPrd5/>.
- [6] Wolfgang Höhle, Yuri Grin, Armin Burkhardt, Ulrich Wedig, Martin Schultheiss, Hans Georg von Schnering, Ralf Kellner, and Herbert Binder. Syntheses, crystal structures, and electronic structure of the boron halides  $\text{B}_9\text{X}_9$  ( $\text{X} = \text{Cl}, \text{Br}, \text{I}$ ). *Journal of Solid State Chemistry*, 133(1):59–67, 1997.
- [7] <https://chemdb.net/en/compound/JEyw7zQyqe/>.
- [8] A. Benrath and B. Schiffrers. Das System Kobaltbromid–Ammoniumbromid–Wasser zwischen  $0^\circ$  und  $100^\circ$ . *Zeitschrift für anorganische und allgemeine Chemie*, 240(1):67–79, 1938.
- [9] Kenji Waizumi, Hideki Masuda, and Hitoshi Ohtaki. X-ray structural studies of  $\text{FeBr}_2 \cdot 4\text{H}_2\text{O}$ ,  $\text{CoBr}_2 \cdot 4\text{H}_2\text{O}$ ,  $\text{NiCl}_2 \cdot 4\text{H}_2\text{O}$  and  $\text{CuBr}_2 \cdot 4\text{H}_2\text{O}$ . cis/trans selectivity in transition metal(ii) dihalide tetrahydrate. *Inorganica Chimica Acta*, 192(2):173–181, 1992.
- [10] Jan Rosdahl, Mikhail Gorlov, Andreas Fischer, and Lars Kloo. Syntheses and crystal structures of di- and trimercury chlorogallates. *Zeitschrift für anorganische und allgemeine Chemie*, 630(5):760–762, 2004.
- [11] T. N. Srivastava, J. E. Griffiths, and M. Onyszczuk. Derivatives of monogermane: Part ii. preparation and properties of germyl pseudohalides and related compounds. *Canadian Journal of Chemistry*, 40(4):739–744, 1962.
- [12] A. B. Venediktov, S. V. Korenev, D. B. Vasil'chenko, A. V. Zadesenets, E. Yu. Filatov, S. N. Mamonov, L. V. Ivanova, N. G. Prudnikova, and E. Yu. Semitut. On preparation of platinum(iv) nitrate solutions from hexahydroxoplatinates(iv). *Russian Journal of Applied Chemistry*, 85(7):995–1002, 2012.
- [13] Ralf Steudel, Klaus Bergemann, Jürgen Buschmann, and Peter Luger. Large sulfur–nitrogen heterocycles: Preparation of the sulfur imides  $\text{S}_n\text{NH}$  ( $n = 8, 9, 11$ ) and structures of  $\text{s}_8\text{NH}$  and  $\text{s}_9\text{NH}$ . *Angewandte Chemie International Edition in English*, 35(21):2537–2539, 1996.
- [14] [https://www.webelements.com/compounds/chlorine/chlorine\\_nitrate.html](https://www.webelements.com/compounds/chlorine/chlorine_nitrate.html).
- [15] A. Lee Smith, William E. Keller, and Herrick L. Johnston. The infrared and raman spectra of condensed nitric oxide. *The Journal of Chemical Physics*, 19(2):189–192, 1951.
- [16] Bernt Krebs, Holger Janssen, Niels J. Bjerrum, Rolf W. Berg, and G. N. Papatheodorou. Niobium aluminum chloride ( $\text{NbAlCl}_8$ ): a molecular dinuclear complex in the solid, melt, and vapor phases. synthesis, crystal structure, and raman spectra. *Inorganic Chemistry*, 23(2):164–171, 1984.
- [17] Neil Bartlett and James Trotter. The structure of the orthorhombic phase of osmium oxide pentafluoride,  $\text{OsO}_5\text{F}_5$ . *J. Chem. Soc. A*, pages 543–547, 1968.
- [18] T. E. Thorpe and A. E. Tutton. Xc.—phosphorous oxide. part ii. *J. Chem. Soc., Trans.*, 59:1019–1029, 1891.
- [19] Th. Kruck and K. Baur. Synthesis of tetrakis(trifluorophosphine)-platinum(0) and tetrakis(trifluorophosphine)-palladium(0). *Angewandte Chemie International Edition in English*, 4(6):521–521, 1965.
- [20] <https://www.lookchem.com/Phosphorus-oxybromide/>.
- [21] Philip Clare, Trevor J. King, and D. Bryan Sowerby. Crystal structures of cis-2,4,6-trichloro- and cis-2,4,6-tribromo-2,4,6-trifluorocyclotri(phosphazene). *J. Chem. Soc., Dalton Trans.*, pages 2071–2074, 1974.
- [22] P. M. Treichel, Ruth A. Goodrich, and S. B. Pierce. Synthesis and characterization of  $\text{HPF}_4$  and  $\text{H}_2\text{PF}_3$ . *Journal of the American Chemical Society*, 89(9):2017–2022, 1967.
- [23] V. Kaiser and F. Menzel. Crystal structure of 2,4-bis(methylthio)-1,3-dithiaphosphetane-2,4-disulfide,  $(\text{CH}_3\text{S})_2(\text{P}_2\text{S}_2)_2$ . *Zeitschrift für Kristallographie - Crystalline Materials*, 206(1-2):279–280, 1993.
- [24] Werner Storzer, Dietmar Schomburg, Gerd-Volker Rösenthaller, and Reinhard Schmutzler. Darstellung und strukturbestimmung von Ammoniak-phosphorpentafluorid (1/1). *Chemische Berichte*, 116(1):367–374, 1983.
- [25] Robert R. Holmes and Raymond N. Storey. Pentacoordinated molecules. viii. preparation and nuclear magnetic resonance study of  $\text{Pb}_2\text{F}_3$  and  $\text{PbF}_3$ . *Inorganic Chemistry*, 5(12):2146–2150, 1966.
- [26] Thomas L. Charlton and Ronald G. Cavell. Preparation and characterization of hydrothiophosphoryl difluoride and hydrophosphoryl difluoride. *Inorganic Chemistry*, 6(12):2204–2208, 1967.
- [27] T. J. Mao, R. D. Dresdner, and J. A. Young. The novel synthesis of  $(\text{PF}_2)_3$  and  $(\text{PF}_2)_4$  from  $\text{P}_3\text{N}_5$ . *Journal of the American Chemical Society*, 81(5):1020–1021, 1959.
- [28] Monika Paulus and Gerhard Thiele. Schwefeldichlorid als Ligand. die Molekül- und Kristallstrukturen von trans-bis(dichlorsulfan)platin(iv)-chlorid  $\text{PtCl}_4(\text{S}_2\text{Cl}_2)_2$  und trans-bis(dichlorsulfan)palladium(ii)-chlorid  $\text{PdCl}_2(\text{S}_2\text{Cl}_2)_2$ . *Zeitschrift für anorganische und allgemeine Chemie*, 588(1):69–76, 1990.
- [29] V.B. Rybakov, L.A. Aslanov, S.V. Volkov, A.V. Grafov, V.I. Pekhn'ov, and Z.A. Fokina. X-ray diffraction study of palladium (2) chlorochalcogenide complexes. *Zhurnal Neorganicheskoi Khimii*, 36(5):1197–1201, 1991.
- [30] [https://www.chemsrc.com/en/cas/13768-11-1\\_1195391.html](https://www.chemsrc.com/en/cas/13768-11-1_1195391.html).
- [31] Christian Wagner, Frank Herzog, Jutta Knaut, and Gerhard Thiele.  $\text{Ru}_4\text{Cl}_{12}$  und  $\text{Ru}_2\text{S}_6\text{Cl}_{16}$ , zwei neue Ruthenium(ii)-Komplexe mit

- scl<sub>2</sub>-liganden. *Zeitschrift für anorganische und allgemeine Chemie*, 625(2):279–284, 1999.
- [32] A. J. Blake and Z. Žák. Structure of disulfuryl difluoride at 100 K. *Acta Crystallographica Section C*, 49(1):7–9, Jan 1993.
- [33] D. P. Stevenson and Robert A. Cooley. The structure of thionyl bromide. *Journal of the American Chemical Society*, 62(9):2477–2479, 1940.
- [34] Jack G. Ballard, Thomas Birchall, and David R. Slim. Preparation of antimony(v) trichloride difluoride and its characterization by means of x-ray crystallography, antimony-121 mössbauer, and raman spectroscopy. *J. Chem. Soc., Dalton Trans.*, pages 1469–1472, 1977.
- [35] <https://de.wikipedia.org/wiki/Diselendibromid>.
- [36] John C. Dewan and Anthony J. Edwards. Fluoride crystal structures. part 27. seleninyl difluoride at –35 °c. *J. Chem. Soc., Dalton Trans.*, pages 2433–2435, 1976.
- [37] K. W. Törnroos, G. Calzaferri, and R. Imhof. Octachlorosilasesquioxane, Cl<sub>8</sub>Si<sub>8</sub>O<sub>12</sub>. *Acta Crystallographica Section C*, 51(9):1732–1735, Sep 1995.
- [38] Cecil L. Frye and Ward T. Collins. Oligomeric silsesquioxanes, (hsio<sub>3/2</sub>)<sub>n</sub>. *Journal of the American Chemical Society*, 92(19):5586–5588, 1970.
- [39] Alois Haas, Reiner Hitze, Carl Krüger, and Klaus Angermund. Darstellung und charakterisierung von silathia- und silasela-grundkörpern / synthesis and characterisation of silathia and silasela basic compounds. *Zeitschrift für Naturforschung B*, 39(7):890–896, 1984.
- [40] H.J. Emeléus, A.G. MacDiarmid, and A.G. Maddock. Sulphur and selenium derivatives of monosilane. *Journal of Inorganic and Nuclear Chemistry*, 1(3):194–201, 1955.
- [41] D. W. S. Chambers and C. J. Wilkins. 982. chlorosiloxanes from the reaction between oxygen and silicon tetrachloride. *J. Chem. Soc.*, pages 5088–5091, 1960.
- [42] H. J. Emeléus and A. G. Maddock. 77. derivatives of monosilane. part iii. the fluoromonosilanes. *J. Chem. Soc.*, pages 293–296, 1944.
- [43] <https://chemdb.net/en/compound/JLrnWwJRbw/>.
- [44] A. Yu. Timoshkin, T. N. Sevast'yanova, E. I. Davydova, A. V. Suvorov, and H. F. Schaefer. Quantum-chemical study of the adducts of silicon halides with nitrogen-containing donors: I. adducts with ammonia. *Russian Journal of General Chemistry*, 72(10):1576–1585, 2002.
- [45] Maxim N. Sokolov, Artem L. Gushchin, Pavel A. Abramov, Alexandr V. Virovets, Eugenia V. Peresyphkina, Svetlana G. Kozlova, Boris A. Kolesov, Cristian Vicent, and Vladimir P. Fedin. Synthesis and structure of ta<sub>4</sub>s<sub>9</sub>br<sub>8</sub>. an emergent family of early transition metal chalcogenide clusters. *Inorganic Chemistry*, 44(24):8756–8761, 2005.
- [46] H. Preiss. Die kristallstruktur von tacl<sub>4</sub>f. *Zeitschrift für anorganische und allgemeine Chemie*, 346(5-6):272–278, 1966.
- [47] J.C. Jumas, M. Maurin, and E. Philippot. Sur les composés fluo et oxyfluo du tellure (iv) : Synthèse, caractérisation et étude structurale de l'acide trioxotetrafluoroditellurique (iv), h<sub>2</sub>te<sub>2</sub>o<sub>3</sub>f<sub>4</sub>. *Journal of Fluorine Chemistry*, 8(4):329–340, 1976.
- [48] J. Weiss and M. Pupp. Mitteilung über Interchalkogen-Verbindungen. II. Die Kristall- und Molekülstruktur von 8,8-Dichlor-1,2,3,4,5,6,7,8-heptathiatellur(IV)-ocan, Cl<sub>2</sub>TeS<sub>7</sub> und von 8,8-Dibrom-1,2,3,4,5,6,7,8-heptathiatellur(IV)-ocan, Br<sub>2</sub>TeS<sub>7</sub>. *Acta Crystallographica Section B*, 28(12):3653–3655, Dec 1972.
- [49] Xiaoli Wang, Yanchao Wang, Maosheng Miao, Xin Zhong, Jian Lv, Tian Cui, Jianfu Li, Li Chen, Chris J. Pickard, and Yanming Ma. Cagelike diamondoid nitrogen at high pressures. *Phys. Rev. Lett.*, 109:175502, Oct 2012.
- [50] R. Blachnik and A. Hoppe. Präparation und thermochemische untersuchung von verbindungen der systeme phosphor-schwefel und phosphor-selen. *Zeitschrift für anorganische und allgemeine Chemie*, 457(1):91–104, 1979.
- [51] K.S. Liang. Local atomic arrangement and bonding studies in amorphous as<sub>2</sub>se<sub>3</sub>–as<sub>4</sub>se<sub>4</sub>. *Journal of Non-Crystalline Solids*, 18(2):197–207, 1975.
- [52] Siegfried Pohl, Ulrich Seyer, and Bernt Krebs. Sulfidhalogenide des germaniums: Darstellung und strukturen von ge<sub>4</sub>s<sub>6</sub>br<sub>4</sub> und ge<sub>4</sub>s<sub>6</sub>i<sub>4</sub> / thiohalides of germanium: Preparation and structures of ge<sub>4</sub>sebr<sub>4</sub> and ge<sub>4</sub>si<sub>4</sub>. *Zeitschrift für Naturforschung B*, 36(11):1432–1443, 1981.
- [53] Silvia Haupt and Konrad Seppelt. Solid state structures of ascl<sub>5</sub> and sbcl<sub>5</sub>. *Zeitschrift für anorganische und allgemeine Chemie*, 628(4):729–734, 2002.
- [54] Farhad Tamadon and Konrad Seppelt. The elusive halides vcl<sub>5</sub>, molcl<sub>6</sub>, and recl<sub>6</sub>. *Angewandte Chemie International Edition*, 52(2):767–769, 2013.
- [55] Joanna Supel and Konrad Seppelt. Rhenium trichloride dioxide, reo<sub>2</sub>cl<sub>3</sub>. *Angewandte Chemie International Edition*, 45(28):4675–4677, 2006.